https://doi.org/10.5194/amt-2023-55
Preprint. Discussion started: 17 April 2023

Atmospheric Measurement Techniques Discussions

A flexible device to produce a gas stream with precisely controlled water vapour mixing ratio and isotope composition based on microdrop dispensing technology

Harald Sodemann[1,2], Alena Dekhtyareva[1,2], Alvaro Fernandez[2,3,4], Andrew Seidl[1,2], and Jenny Maccali[2,3,5]

[1]Geophysical Institute, University of Bergen, Norway
[2]Bjerknes Centre for Climate Research, Bergen Norway
[3]Geoscience Department, University of Bergen, Norway
[4]Andalusian Institute of Earth Sciences, CSIC-University of Granda, Spain
[5]SFF Centre for Early Sapiens Behaviour (SapienCE), University of Bergen, Norway

Correspondence: Harald Sodemann (harald.sodemann@uib.no)

Abstract. Here we describe a versatile device to produce a flow of air-vapour mixture with controlled humidity and water isotope composition based on microdrop dispensing technology. By precisely controlling the contribution of water from two dispenser heads into a carrier gas stream, the device allows to set the air-vapour stream to any isotope ratio between two end member waters. In addition to presenting the design and several performance characteristics of the new system, we describe two application examples. First, we utilize the device to determine a common artifact of vapour isotope analyzers, known as the mixing ratio – isotope ratio dependency. Second, we utilize the device to provide a constant background stream of humid air for fluid inclusion water isotope analysis in stalagmites. The observed flexibility and precision of the device underpints its usefulness and potential for a wide range of applications in atmospheric water vapour isotope measurement applications. Future improvements could focus on reducing the number of manual interventions and improved control at high flow rates.

1 Introduction

The composition of stable water isotopes in ocean and surface waters, land ice, and precipitation has long been used to extract valuable information about the climate system (Horita et al., 2008; Galewsky et al., 2016). Since the advent of instruments based on Cavity-Ring Down Spectroscopy (CRDS) for water isotope analysis (Kerstel et al., 2006; Lee et al., 2005; Gupta et al., 2009), water vapour can be measured continuously at a time scale of seconds, providing for example insight into the details of weather systems (e.g., Graf et al., 2019). To match the precision and accuracy of IRMS, laser-based isotope analysers need frequent calibration of the raw data to account for instrumental drift, as well as characterisation of analyzer properties (Sturm and Knohl, 2010; Aemisegger et al., 2012) Currently, the variability of the calibration system, together with inlet and instrument characteristics, is an important contributor to the total uncertainty of atmospheric water vapour isotope measurements, in particular at low humidities (Sodemann et al., 2017; Seidl et al., 2023). For example, Weng et al. (2020) showed a dependency of the raw signal of CRDS analyzers on both mixing ratio and isotope ratio of the measured vapour, which is different for

https://doi.org/10.5194/amt-2023-55
Preprint. Discussion started: 17 April 2023


Atmospheric Measurement Techniques Discussions

every analyzer. Correction functions for this dependency require a detailed characterisation of each analyzer, obtained from the provision of a precise air-vapour stream with defined mixing ratio and isotope composition over sufficiently long averaging times by means of an external vapourisation device.

The characteristics and properties of such an external vapourisation device are critical to obtain accurate and precise measurements of the water vapour isotope composition. A range of devices with distinct designs have so far been used to generate a vapour stream for instrument characterisation and calibration. The bubbler design consists of a dry air stream that is percolated through a sufficiently large water reservoir at a defined temperature. The emanating vapour contains then an isotope composition in isotopic equilibrium with the liquid for the given temperature (e.g., St Clair et al., 2008). There are several drawbacks of such a bubbler design. First, the isotope composition will drift over time, as more water evaporates, requiring repeated liquid samples to monitor the isotope composition of the water reservoir. Furthermore, the production of vapour with mixing ratios below dew point of 0 °C at standard pressure will involve additional mixing with dry air, and the temperature of the liquid needs to be precisely regulated.

Another design concept to circumvent complications from isotope fractionation involves the complete evaporation of liquid water into a heated cavity. Such systems are for example commonly used for liquid sample analysis, where an autosampler injects about 2 μl of water into a cavity heated to 110 °C (e.g., van Geldern and Barth, 2012). Such systems only produce a vapour stream of a few minutes duration, which is sufficient for liquid sample analysis, but not sufficient for longer-term instrument characterisations. Another design that allows for generation of a continuous vapour stream with complete evaporation is based on a nebulizer head is the water vapour isotope standard source (WVISS, Los Gatos Research, USA). The WVISS allows for production of a vapour stream over several hours for one standard at a time. In addition to manual intervention for changing standards, the system requires external modifications to reach lower mixing ratios, and the achieved precision of the vapour signal can be a limitation for some applications (Aemisegger et al., 2012).

A further design concept is to continuously inject a small amount of standard water into a heated cavity by means of thin needles, such as used in the Standard Delivery Module (SDM, Picarro Inc, Sunnyvale, USA). Built as an external module added to the liquid water analysis setup of these analyzers, the SDM provides a vapour stream at a typical flow of 35 sccm, supplied from water standard reservoirs by two syringe pumps. The mechanically operated syringe pumps are prone to failure of moving parts, and air bubbles in the lines can lead to strong oscillations in the mixing ratio, requiring manual intervention. Both can be important limitations for calibration in remotely-operated measurement setups (Bonne et al., 2014). A further design with complete evaporation that has been used for example in providing a constant background humidity in fluid inclusion analysis involves a peristaltic pump that delivers a water droplets into an N_2 gas stream heated to 140 °C (Affolter et al., 2014). A similar design has been used in the continuous analysis of water from ice cores on a melting bed, where the liquid is provided through a capillary to a heated oven (Gkinis et al., 2010). Both designs have only limited possibility to regulate the mixing ratio of water vapour in the airflow, but have been operated over extended time ranges (Bonne et al., 2019).

A design concept with complete evaporation of standard water and fine-grained control of the mixing ratio is based on the dispension of micrometer-size droplets (St Clair et al., 2008). Microdrop systems are essentially ink jet printer heads that eject droplets from a glass capillary at a defined size by means of piezoelectric stimulation. Thereby, the head is filled or

https://doi.org/10.5194/amt-2023-55
Preprint. Discussion started: 17 April 2023


Atmospheric Measurement Techniques Discussions

emptied by pressure applied to the head space of the reservoir. During dispensing of droplets, the liquid is supplied to the printer head by capillary forces. The particular advantages of a microdrop system in the context of vapour stream generation is the precise control of the amount of water released from the dispenser head by modification of voltage and frequency (Iannone et al., 2009). Release of individual water droplets at a defined size enables fast and complete evaporation without fractionation artefacts. Sayres et al. (2009) applied a bubbler and a microdrop system with a high flow rate of dry gas (100 slm) to achieve a stable flow at low humidity (<200 ppmv) needed for calibration of cavity-based absorption instrument used for upper troposphere and lower stratosphere measurements. Sturm and Knohl (2010) built a prototype vapour generator based on microdrop technology, that required manual change of standards, but the technology has not been developed further since. Therefore, there is currently no single system available that in combination provides a precise stream of water vapour across a range of mixing ratios, flow rates, and different stable isotope compositions.

Here we present a new, versatile calibration system for CRDS vapour isotope analyzers based on microdrop dispensing technology, allows to produce a precise vapour stream over a range of mixing ratios and flow rates. As a key innovation, we use two dispensing heads simultaneously, providing to our knowledge the first system that allows to generate a vapour stream with any isotope composition along the mixing line of two standards. Due to its flexibility, the device is suitable for a range of applications, including instrument characterisation, calibration of water vapour isotope measurements, and as a component in specific laboratory applications. In addition to presenting the design and performance characteristics of the new system, we describe two different application examples of increasing complexity, namely the characterization of the mixing ratio – isotope ratio dependency of CRDS analysers, and the provision of background humidity for stalagmite fluid inclusion isotope analysis.

2 Application requirements, design objectives, and specifications

We designed the device for vapour generation in a way that would allow for a wider range of applications with CRDS analyzers than possible with any single currently available device. Such applications include (i) providing a background humidity for fluid inclusion water isotope analysis. In this application, a vapour stream with precise mixing ratio (SD(30 min)<20 ppmv) at a set isotope composition should be provided for several hours to days. (ii) Providing a vapour stream for calibration with flow rates between 35 and 250 sscm. This range of flow rates is required to produce the vapour stream required by analyzers that run in different flow configurations, such as the standard low-flow configuration of Picarro analyzers at 35 sscm, and the flux configuration with flow rates of about 150 sccm for aircraft measurements (Sodemann et al., 2017). Even larger flow rates allow to characterize the response times of inlet lines with additional flush pumps used in semi-permanent installations for water isotope analysis (e.g., Steen-Larsen et al., 2013; Bonne et al., 2014; Galewsky et al., 2016). (iii) Providing a wide range of isotope composition and mixing ratios for instrument characterisation. Characterisation of analysers in terms of their mixing ratio – isotope ratio dependency requires to independently step through mixing ratio and isotope composition (Weng et al., 2020). This is facilitated greatly by an on-line, adjustable mixing of the evaporated water between two end-member standards. To cover the typical ambient mixing ratios encountered in mid-to high latitudes from the surface to high-elevations, the range

https://doi.org/10.5194/amt-2023-55
Preprint. Discussion started: 17 April 2023


Atmospheric Measurement Techniques Discussions

of mixing ratios should encompass at least 500 to 25000 ppmv. Furthermore, the entire system should be small and robust enough to be portable to a field location, for example by fitting into a standard 19-inch rack size.

These requirements, in their combination, are not met by any existing calibration system, and would require either a combination of or modification to currently available systems. In particular the ability to set the isotope composition within a range is not available from current devices. For example, the SDM provides a more limited range of humidities, with at least 6000 ppmv, and at most 20 min of operation, before a new cycle is started. The SDM is also limited to two standard waters and allows no easy exchange or mixing of different standards. Injections with the autosampler are feasible with a specific method. Mixture of different standards is also possible before starting the autosampler. However, the mixtures have to be analysed beforehand, or one has to use several lab standards that have been calibrated beforehand.

3 Device components and setup

At its core, the calibration device consists of a vertical evaporation chamber where the vapour stream is generated (Fig. 1). The evaporation chamber is a custom modification of a 300 ml sample cylinder (Swagelok Inc., USA, Part No. 304L-HDF4-300-T) with 1/4 inch NPT threads on both ends. Two stainless steal tubes of 30 mm length and 10.1 mm inner diameter have been welded horizontally to the upper part of the evaporation chamber, facing each other at an angle of 60 °C and with a vertical offset of 10 mm. The two tubes reach 3 mm into the interior of the chamber, and each holds a dispenser head (Microdrop GmbH, Germany, Part Nr. MK-K-130). Each dispenser head (DH) is connected to one 12 ml glass vial mounted next to the evaporation chamber that holds a liquid water standard. Both DHs and the standard vials are connected to a control device that among other parameters controls the piezo-electric pulse voltage and duration, the pulse frequency, and headspace pressure for both DHs. In order to reduce the retention time of water vapour in the evaporation chamber, the assembly has been treated with a hygrophobic coating (SilcoNert, SilcoTec Inc., USA).

Dry air (synthetic air) or N_2 is introduced as a carrier gas at the lower end of the evaporation chamber. The carrier gas is heated during passage of 60 cm of 1/4 inch SS tubing that bends between two brass plates that are heated on the outside by heat trace covered with metal mesh (Watcom Inc, USA). The heat trace wraps around both the gas heating assembly and the evaporation chamber, and is controlled to 60 °C. Temperatures near the DHs are monitored to remain below 60 °C to minimize evaporation of liquid directly from the DH, which could possibly interrupt the dispensing.

A manual valve provides either N_2 or dry air from a gas tank or other source to the calibration unit. At the entry into the heated tubing, a mass flow controller (GFC 17, Alborgh Inc, USA) regulates the flow rate electronically to a set value between 0 and 500 sccm. The experiments presented here were either performed with high-purity grade N_2 (Nitrogen 5.0, purity >99.999 %; Praxair Norge AS, x<5 ppmv), synthetic air (synthetic air 5.5, purity 99.9995 %; Praxair Norge AS, x<5 ppmv), or air sourced from a dry air generator with added drying cartridges (MT-400, VWR, USA, m<100 ppmv). Typically, the carrier gas was supplied with a pressure of <1 bar upstream of the mass flow controller.

At the upper outlet of the evaporation chamber, different applications tap the vapour stream from a 1/4 inch SS connection with Swagelok compression fitting. Depending on the application, the vapour stream was directly provided to the CRDS

https://doi.org/10.5194/amt-2023-55
Preprint. Discussion started: 17 April 2023

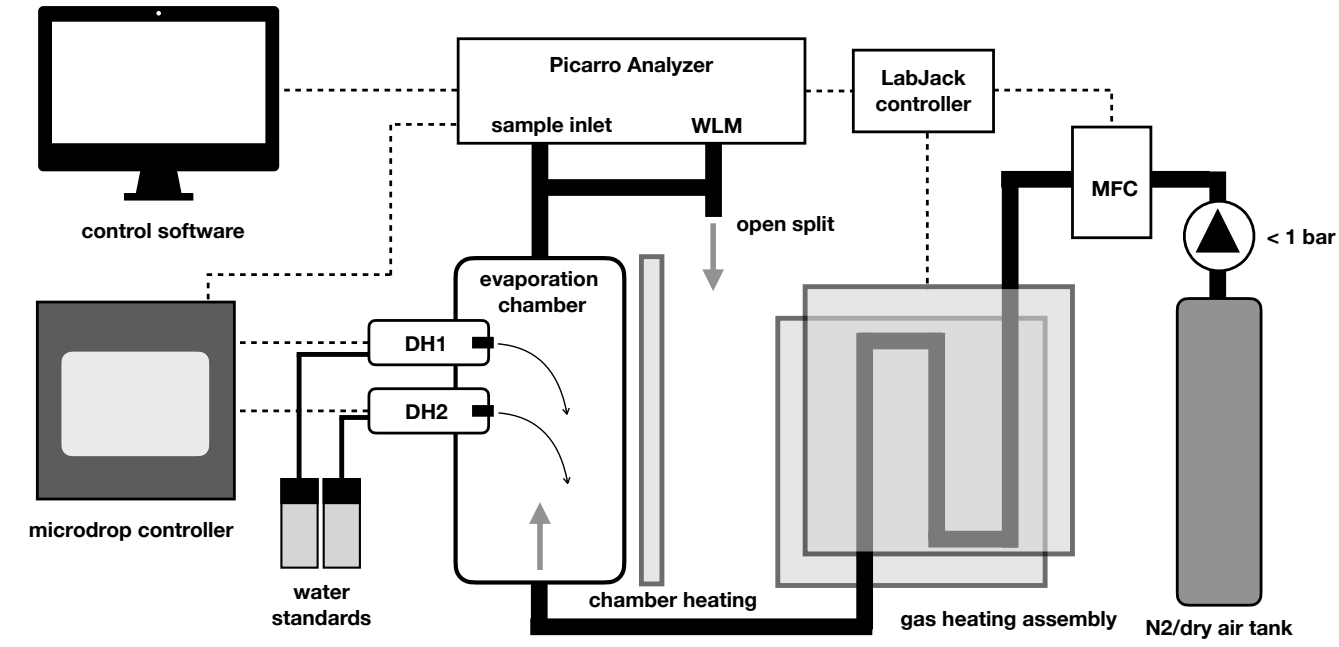

Figure 1. Schematic of the microdrop calibration device components. Thick black lines indicate tubing for gas flow. Dashed lines indicate electrical signal flow. For further details see text.

analyzer, or lead into an analytical assembly upstream of the analyzer. Typically, an open split allowed for excess vapour to be vented into the room, with a line leading to the Wave-Length Monitor (WLM) port of the Picarro analyzers.

A custom software written in python running on the Picarro analyzer controls the flow rate of the mass-flow controller, the dispenser heads, and temperatures via a digital/analog interface (U12, LabJack Inc., USA). The software allows to manually fill, empty and modify settings for each DH, including dispension frequency, and to step through an automated sequence with a specific frequency at which each dispenser head injects droplets into evaporation chamber.

4 Operating principle and procedures

The operating principle of the microdrop calibration device is based on the precisely controlled injection of liquid water into the evaporation chamber. The number of droplets of a specific size ejected into the evaporation chamber, which is flushed at a specific flow rate, results in a moist air stream with a water vapour and isotope ratio adjusted to the desired application.

https://doi.org/10.5194/amt-2023-55
Preprint. Discussion started: 17 April 2023

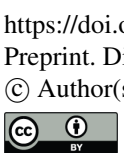

Atmospheric Measurement Techniques Discussions

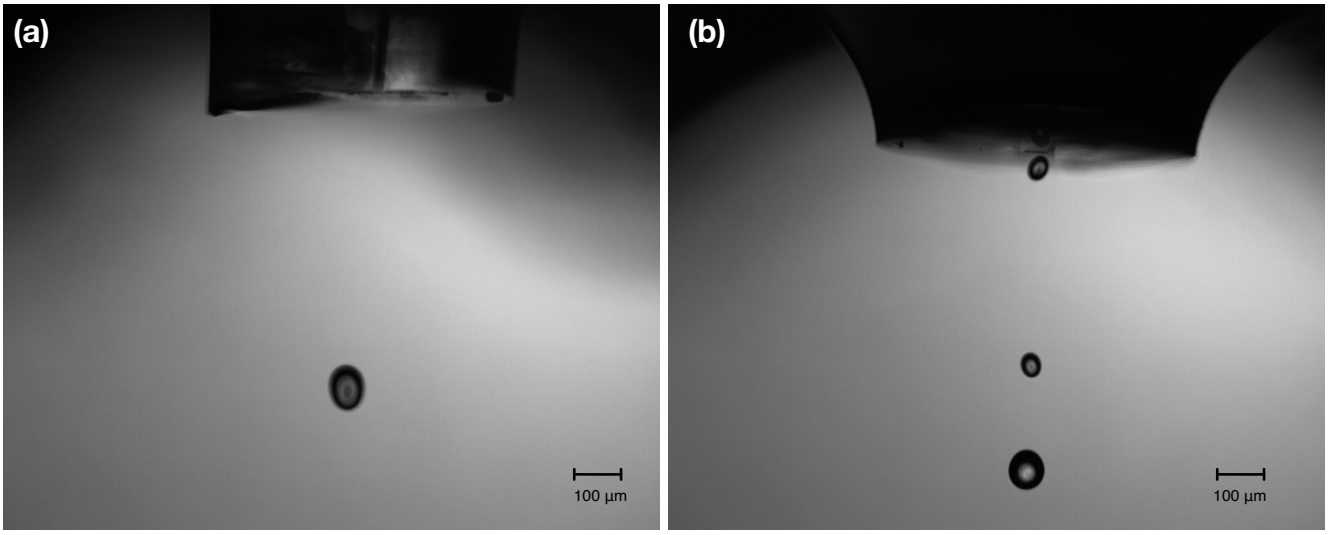

Figure 2. Pictures of heads with scale, well-formed and jet-like drop examples. (a) Single drop emanating from DH with serial number 1016 at 85 V and 16 μs pulse width. (b) Jet-like drops emanating from DH with serial number 1015 with 85 V and a pulse width of 100 μs.

4.1 Droplet generation and droplet evaporation

The microdrop dispensing technology with the DHs used here allows to generate droplets with diameters ranging between 35.0 to 90.0 μm in diameter, depending on fluid properties (Table 2). The droplets can be ejected from the nozzle into the evaporation chamber with frequencies between 1 and 1500 Hz. As the droplets are ejected with about 2 ms^{-1} into the heated dry carrier gas flow, they rapidly evaporate before reaching the bottom of the evaporation chamber. The drop size range is more limited than the theoretically available range of drop sizes, as it depends on the nozzle diameter, fluid viscosity, and piezoelectric pulse voltage and duration parameters. We observed that, in line with manufacturer specifications, only at specific combinations of settings for the piezo-electric pulses (defined by voltage and duration) a single droplet, rather than a jet or sequence of drops was ejected. Higher voltages thereby tended to provide a droplet stream that operated over longer times before it could stop randomly. The piezo-electric parameters needed to be determined for each DH in a relatively time-consuming procedure using a separate setup with a high-speed camera. Figure 2 gives examples for well-formed (panel a) and jet-like (panel b) droplet generation. Drop-like ejection is important for the linearity of the DH performance across frequencies and flow rates (Sec. 4.2). After suitable settings for the drop size had been found, the piezo-electric parameters were not modified further until a decrease of the DH performance was observed, typically after several months. The theoretical limits for the specified rate of flow rates at the given dropsize of about 70 μm are given in Table 1.

https://doi.org/10.5194/amt-2023-55
Preprint. Discussion started: 17 April 2023

Atmospheric Measurement Techniques Discussions

Table 1. Theoretical mixing ratio and relative humidity at 60 °C of the air-vapour stream for a typical range of operating parameters for a drop size of 70 μm.

Frequency (Hz)	Carrier gas flow (sccm)	Mixing ratio (ppmv)	Relative humidity (%)
10	50	795	0.7
10	250	160	0.1
1000	50	79511	72.2
1000	250	15902	14.5

Table 2. Performance characteristics and calibration parameters for 3 MK-K-130 DHs used in the microdrop device.

DH	1	2	3
Serial number	1015	1016	1032
Nozzle diameter	50 μm	50 μm	50 μm
Frequency range	1–1500 Hz	1–1000 Hz	1–1000 Hz
Tubing	10 cm PTFE	10 cm PTFE	11.5 cm PTFE
Calibration voltage	51 V	58 V	54 V
Calibration pulse length	39 μs	23 μs	26 μs
Calibration drop size	68 μm	74 μm	75 μm

4.2 Linearity and effective drop size

As each dispensed drop adds a defined volume of water to the airstream, an ideal DH would provide a linear correspondence between the dispensing frequency and the mixing ratio of the resulting vapour stream. We can use this relation between drop size and mixing ratio to compute the effective drop size of the DHs for a given voltage setting and run. To this end, we first calibrate the raw mixing ratio signal with a calibration curve obtained from a dewpoint hygrometer. Then we compute the mass flux of the carrier gas at a given temperature, and obtain the effective drop size from the water mass contained in the air-gas mixture for a given frequency.

Figure 3 shows the mixing ratio resulting for different DH operating frequencies, using dispersion parameters 82 V, 28 μs for both DH1 and DH2. Both DHs have different performance characteristics, quantified by the slope of a linear fit. DH1 has for the given settings an efficiency of about 200 ppmv Hz^{-1}, compared to 125 ppmv Hz^{-1} for DH2. In addition, some scatter is apparent for both heads that represents day-to-day variability. Importantly, the results in Fig. 3a are obtained for non-ideal disperson settings, where a jet rather than discrete bubbles were ejected from both DHs. If the system is operated using dispersion parameters that lead to single drops, the performance characteristics improve markedly, both in terms of

https://doi.org/10.5194/amt-2023-55
Preprint. Discussion started: 17 April 2023

Atmospheric Measurement Techniques Discussions

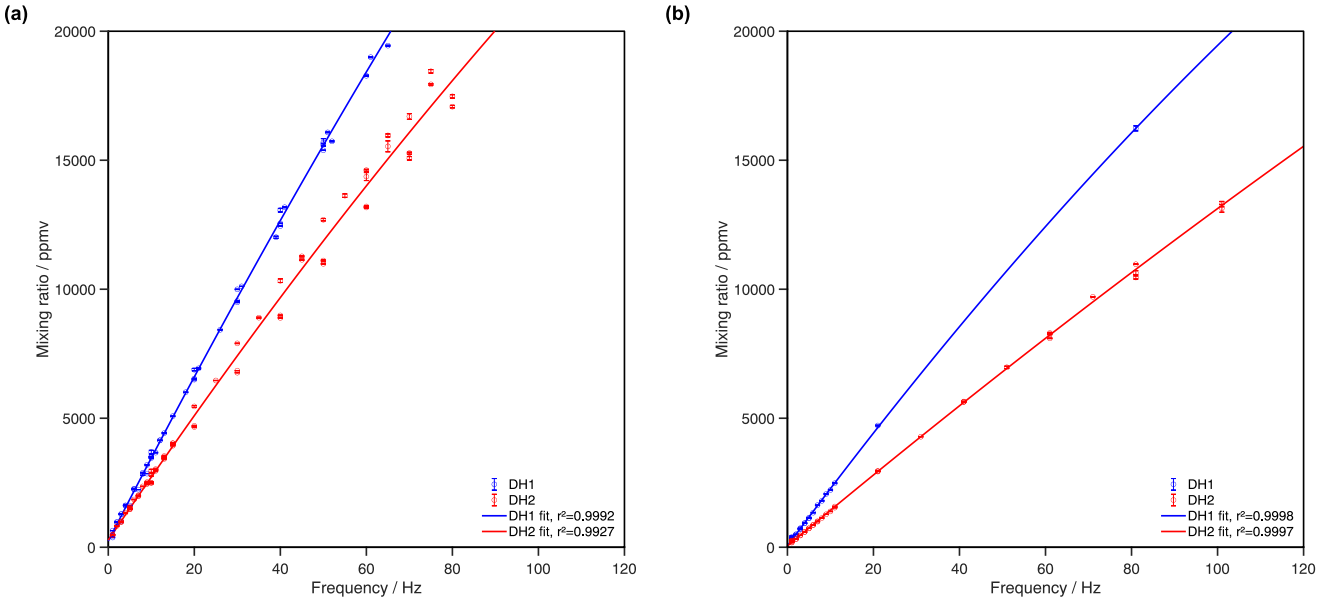

Figure 3. Performance of two dispenser heads at fixed droplet generation parameters and variable frequency. Measurements have been performed on a Picarro L2140-i analyser (serial no. HKDS2038) (a) with dispensing parameters 82V, 28 μs for both DH1 and DH2 and (b) with dispensing parameters 82V, 18 μs for DH1 and 82V, 19 μs for DH2.

linearity (Fig. 3b) and day-to-day reproducibility (Fig. 4). Day-to-day standard deviations of drop size are typically only a few micrometers (Fig. 4, red and blue histogram). Over the entire time period, the variability was substantially larger (Fig. 4, grey histograms). This result demonstantes the need to determine the effective drop size and a suitable dispensing parameters repeatedly over time to control the amount of liquid released from a dispensing head for a given frequency.

4.3 Liquid water standard preparation

The water standards used here are secondary laboratory standards calibrated at FARLAB, University of Bergen on the VSMOW-SLAP scale with primary standard material provided by IAEA, according to their recommendations (IAEA, 2009). We used a depleted standard (GLW, -40.10±0.03 for δ^{18}O; -308.8±0.1 for δ^{2}H) and a standard close to local meteoric waters (DI2, -7.64±0.02 for δ^{18}O; -49.8±0.3 for δ^{2}H). Prior to filling DH reservoirs, the standard waters were filtered using a 0.2 μm PTFE filter (Part No. 514-0066, VWR, USA). This procedure is recommended by the manufacturer to prevent clogging of the DH capillary and PE tubing, and thus damage to the DHs. Furthermore, to prevent the DH from arbitrarily stopping dispensing due to gas bubbles in the capillary, dissolved gas was removed from the liquid by suspension of the vials in an ultrasonic bath for about 15 min.

https://doi.org/10.5194/amt-2023-55
Preprint. Discussion started: 17 April 2023

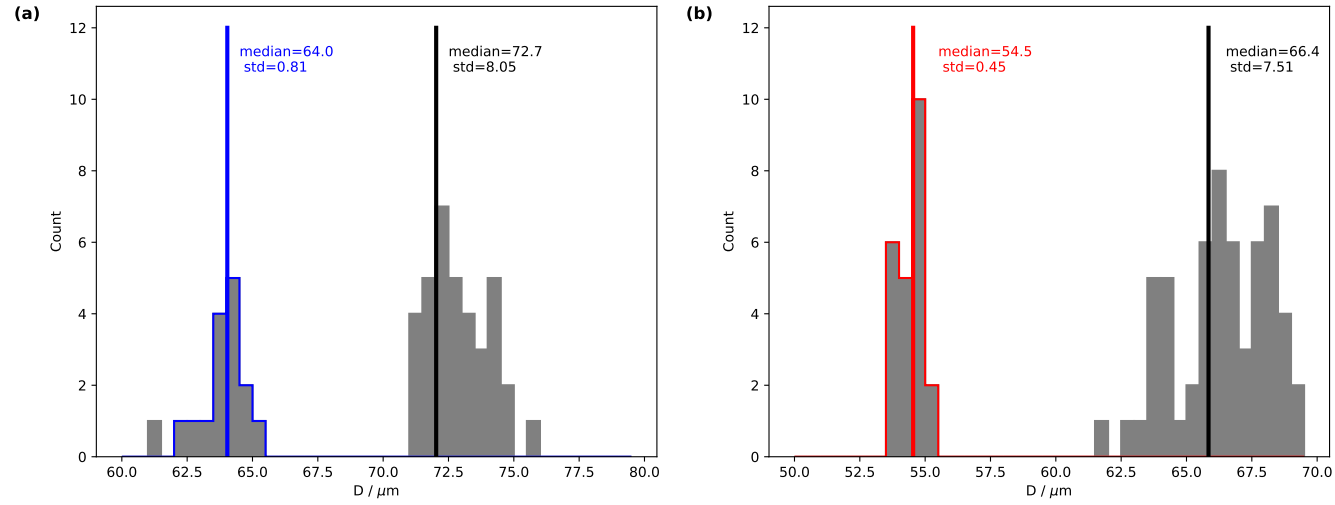

Figure 4. Histograms of droplet size computed from the dispensing parameters (a) for DH1 and (b) for DH2 with all dispersion parameters (grey shading, black median and standard deviation) and only with dispening parameters 82 V, 18 μs for DH1 (blue) and 82 V, 19 μs for DH2 (red).

4.4 Operating procedures

Before producing a vapour stream, the standards need to be filtered and degassed, filled into reservoirs, and the device heated to the operating temperature of 60 °C (typically <30 min) with gas flow enabled (>35 sccm). This heating time will allow the device to reach a residual background mixing ratio of well below 100 ppmv. Thereafter, the standard operating procedures for the calibration device to produce a vapour stream include the following steps:

1. Remove DHs from evaporation chamber
2. Empty and fill DH with standard water using software control, wait for holding pressure to stabilize
3. Test DH operation by ejecting onto a lint-free piece of cloth, lit by a bright light source on a dark background at high dispension frequency (1000 Hz)
4. Stop dispensing and insert DH in evaporation chamber, attach and seal DH
5. Start dispensing at desired frequency from software.

These steps need to be followed at the start of a measurement sequence, but also each time when DH operation stops accidentally (Sturm and Knohl, 2010). Critical aspects during this normal operation sequence, and error sources leading to interruptions or poor calibration system performance are discussed in Sec. 8.

https://doi.org/10.5194/amt-2023-55
Preprint. Discussion started: 17 April 2023

Atmospheric Measurement Techniques Discussions

5 Device characteristics

This section presents typical results for the device characteristics regarding the linearity of the DH performance, stability of the calibration air stream, and ability of the system to generate mixtures of different standard waters at different flow rates.

5.1 Short-term stability

Stability of the water vapour mixing ratio and isotope composition of the calibration device are important in isotope analysis, and need to be quantified. In order to assess stability of the microdrop vapour device across a range of time scales for a continuous period of operation, we use the Allan deviation, which is given by the square root of the Allen variance (e.g., Sturm and Knohl, 2010):

$$\sigma^2(\tau) = \frac{1}{2n}\sum_{i}^{n}(y_i + 1(\tau) - y_i(\tau))^2 \quad (1)$$

hereby, τ is the averaging time, y_i is the average value of measurements in an averaging interval i, and n is the number of averaging intervals for a given averaging time τ.

The minimum of the Allen deviation indicates the optimal averaging time, where the highest measurement precision can be achieved. While primarily a property of the CRDS analyzer, the vapour stream needs to be sufficiently stable to enable analyzer characterisation. Thus, variability of the vapour stream needs to be minimal to identify instrument characteristics, rather than calibration system characteristics from the analysis of the Allen variance. The Allen deviation has been assessed from a constant operation of the microdrop device, dispensing at 65 Hz into a N_2 stream of 70 sccm during about 4 h, resulting in an average mixing ratio of about 18'400 ppmv (Fig. 5). For averaging times below 10 s, the Allen deviation of the mixing ratio is less than 5 ppmv, and remains below 10 ppmv for up to 30 s average times. The maximum variance of about 30 ppmv is reached after 100 s. We compare this to a measurement sequence obtained with the SDM and the same standard with daily calibrations during 25–29 March 2021. In total five calibration sequences have been combined to a 1:45 h time series for the assessment of the Allen deviation of the same analyzer with an SDM (Fig. 5, black lines). Notably, for mixing ratio, the SDM has generally a factor of 5 lower precision than the microdrop device, with an overall minimum of 10 ppmv. For $\delta^{18}O$, the Allen deviation with the SDM is initially lower than for the microdrop device, but reaches a minimum of only 0.05 ‰ after about 4 s, whereas the microdrop provides the highest precision of 0.03 ‰ after about 25 s (Fig. 5b). For δ^2H, the findings are similar, with a minimum in the Allan deviation for the SDM at 4 s with about 0.3 ‰, compared to below 0.2 after 30 s with the microdrop device (Fig. 5c). The results obtained for the microdrop device appear in a similar range as with a capillay vapour generator obtained by Steig et al. (2014) and for the WVIA generated Allan deviation in Aemisegger et al. (2012) for the same type of analyzer, albeit these studies considered much longer measurement periods, and thus achieve a lower minimum at longer averaging times. We note here that the micodrop device is able to provide a vapour stream with properties that allow to determine the precision of the analyzer consistent with literature. The SDM vapour stream used here was substantially

https://doi.org/10.5194/amt-2023-55
Preprint. Discussion started: 17 April 2023

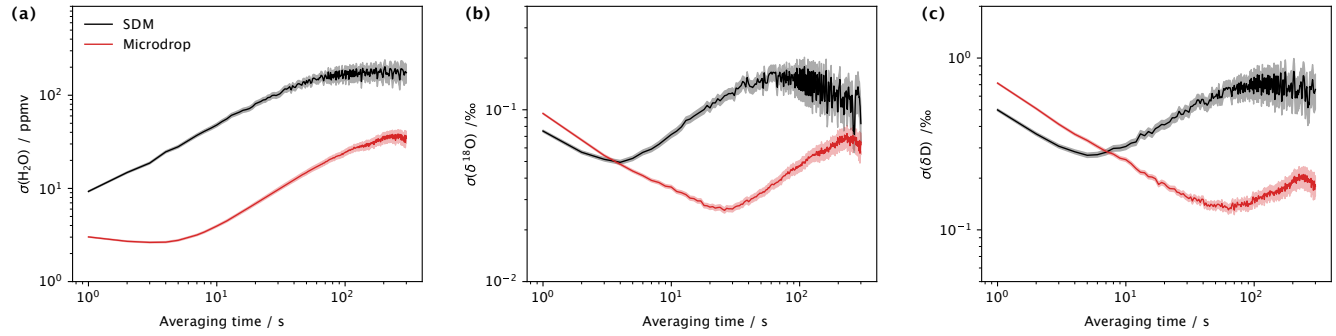

Figure 5. Allen deviation for (a) mixing ratio (ppmv), (b) δ^{18}O (‰) and (c) δ^{2}H (‰) by the microdrop device (red) and an SDM (black) on analyzer HIDS2254 with standard DI2. The microdrop measurements were performed in the laboratory on 08 March 2023. The SDM measurements were combined from a set of shorter daily calibration perids obtained from 25–29 March 2021.

more noisy, and does not appear to be equally useful for analyzer characterisation. It is therefore important to consider the contribution of the vapour generation device when characterising the short-term stability of a CRDS water isotope analyzer.

5.2 Long-term stability

Stable background water vapour mixing ratios and δ^{18}O and δ^{2}H values are particularly important for accurate and precise fluid inclusion data. We evaluated the long-term stability of the microdrop system as part of a crushing line setup (Sec. 7). From 16 analytical sessions with the crushing line over a period of 5 weeks, we obtain H_2O concentrations between 9550 and 13500 ppmv for 37 different occasions (Table A1). We selected a duration of 15 min to calculate short-term stability of each fluid inclusion sample peak measurement in that period (see Sec. 7). As a measure of long-term stability, we find an average standard deviation of 11.6±6.6 ppmv for water mixing ratio, 0.10±0.01 ‰ for δ^{18}O, and 0.65±0.02 ‰ for δ^{2}H values on a 15 min time scale in this humidity range (Fig. 6). These standard deviations are much lower than typical sample peak heights during fluid inclusion measurements (see Sec. 7 and Fig. 13 below) as required for reliable fluid inclusion analysis (Affolter et al., 2014; Dassié et al., 2018; de Graaf et al., 2020). The long-term stability obtained here is also in a similar but slightly larger range as the short-term stability (Fig. 5). The larger variability on longer time scales can be induced by different factors in the analytical line setup and the microdrop device, including variation in dispensor head performance, build-up of residual in the crusher line, and other factors (Sec. 7 and 8).

5.3 Variation of carrier gas flow rate

The mass flow controller allows to regulate the flow rate in a range of 0–500 sccm. When using a Picarro L2140-i analyzer, or similar, in low-flow mode, at least 50 sccm of gas flow are required to avoid leakage of ambient air from the open split. Importantly, with faster gas flow, the residence time of the vapour stream in the microdrop device decreases, and becomes potentially turbulent in the evaporation chamber. Thus, faster flow rates can lead to better mixing conditions, and offset the

https://doi.org/10.5194/amt-2023-55
Preprint. Discussion started: 17 April 2023

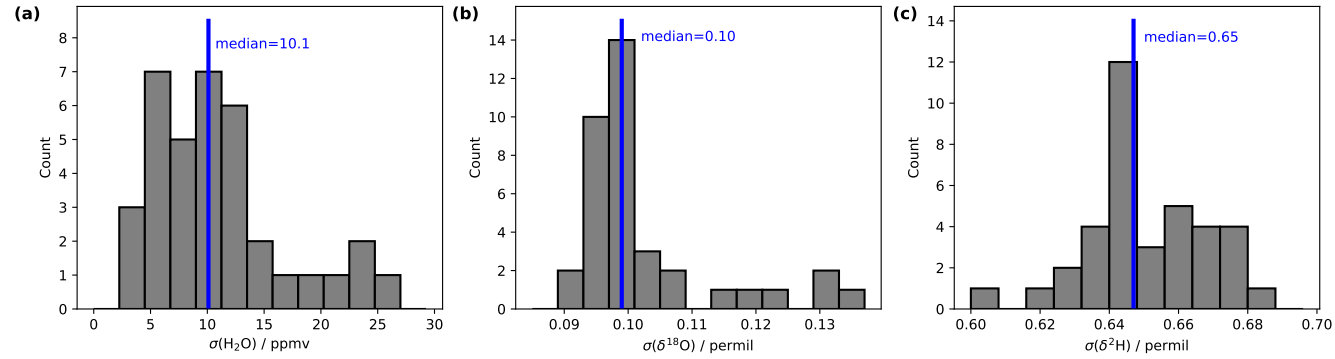

Figure 6. Long-term stability of the vapour stream assessed during a range of measurement days in Oct-Nov 2020. Histograms show standard deviations on (a) water vapour mixing ratios (ppmv), (b) δ^{18}O (‰) and (c) δ^{2}H (‰) values, calculated over 15 min long time intervals (n=37).

fall of droplets to a larger degree. On the other hand, slight overpressure may build up in the evaporation chamber, which counteracts the operation of the DH. We therefore investigated the performance of the device in terms of the Allan deviation (Eq. 1) for water vapour and the isotope composition at three different flow rates. To this end, DH1 was operated with laboratory standard DI2 for about 3-hour long segments with N_2 flow rates of 70, 140 and 250 sccm, and dispensing frequencies of 120, 210 and 350 Hz during 08–12 March 2022. The mixing ratio in all three setups was between 18'000 and 20'000 ppmv . The Allan deviation for 70 and 140 sccm is very similar for both mixing ratio (Fig. 7a) and the two isotope values (Fig. 7b,c). At averaging times of 30 s and longer, the Allan deviation becomes about 2 times larger for 140 sccm (black line) than 70 sccm (red line). At a flow rate of 250 sccm (blue line in Fig. 7), the Allan deviation is larger for the mixing ratio throughout the range of averaging times (Fig. 7a), while for both isotope species, the Allan deviation only increases for averaging times of more than 10 s. This indicates that the microdrop device can produce a usable vapour stream at flow rates of up to 250 sccm. However, the mixing ratio is more variable, and an additional mixing chamber may be required downstream to further stabilise the vapour stream.

5.4 Mixing of water from two dispenser heads

With the presence of two DHs dispensing water standards that have large differences in isotopic composition, it is possible to produce a vapour stream that is freely mixed from simultaneously operating two heads. We have tested the linearity of the mixing across a range of frequency settings using standards DI2 and GLW. Using frequency ratios $r = \mathrm{DH2}/(\mathrm{DH1} + \mathrm{DH2})$ of 0.0, 0.2, 0.3, 0.4, 0.5, 0.6 and 1.0, we step through a range of frequencies for both dispenser heads. For example, to obtain a mixing ratio of 5000 ppmv at $r = 0.2$, we dispense with a frequency of 5 Hz from DH2 and 20 Hz from DH1 (ignoring sensor head efficiency for simplicity at this point). The linearity of this mixing is provided over a range of mixing ratios (Fig. 8a). Thereby, the efficiency of the dispenser heads needs to be taken into account for precisely regulating the mixture (Sec. 4.2). At lower humidity than 5000 ppmv, deviations from the linear mixing become apparent (Fig. 8b). These deviations are however

https://doi.org/10.5194/amt-2023-55
Preprint. Discussion started: 17 April 2023

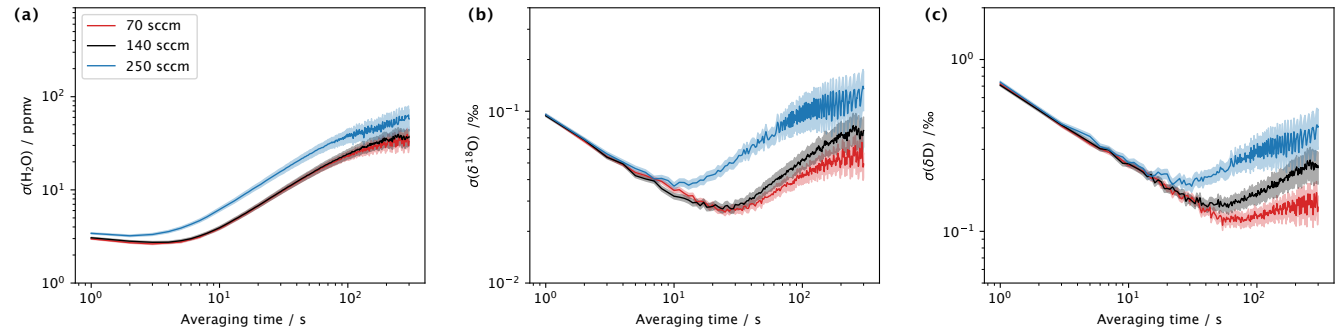

Figure 7. Comparison of Allan deviation for (a) water vapour mixing ratio (ppmv), (b) δ^{18}O (‰), and (c) δ^{2}H (‰) at flow rates of 70 sccm (red), 140 sccm (black), and 250 sccm (blue) obtained from a sequence of measurements at mixing ratios of 18'000-20'000 ppmv during March 2022.

not due to the changes in the dispensing frequency, but rather an effect of the mixing ratio – isotope ratio dependency (Weng et al., 2020). As in the results of Weng et al. (2020), obtained from liquid injections and SDM measurements, the humidity dependency varies with isotope ratio and isotope species at mixing ratios below about 5000 ppmv. This is for example seen when comparing the raw δ^{18}O signals bending downward for Mix000 and upward for Mix100 at below 5000 ppmv. By varying the dispensing frequency at a fixed frequency ratio, and in addition changing the flow rate, a vapour stream with given isotope ratio can be produced over a wide range of mixing ratios. Thus, the microdrop vapour generator can be used to quantify the mixing ratio – isotope ratio dependency for nearly arbitrary positions in the mixing ratio – isotope ratio space (Sec. 6).

6 Application 1: Characterisation of the isotope composition-mixing ratio dependence of CRDS analyzers

We now present a first application example where the microdrop vapour generator is directly connected to the analyzer. In this application example, we exploit the capability of the calibration system to modify both mixing ratio and isotope ratio, and thus obtain a detailed characterisation of the mixing ratio – isotope ratio dependency (Weng et al., 2020). This measurement artefact results from the performance of Picarro L2130-i and L2140-i CRDS analysers being optimized for liquid sample analysis at a water vapour mixing ratio of approximately 20000 ppmv. If the analyzer samples air or nitrogen at water vapour mixing ratios below about 5000-10000 ppmv, the measurements need to be corrected for this artefact. Earlier studies detected this as a mixing ratio dependency (Lis et al., 2007; Sturm and Knohl, 2010; Steen-Larsen et al., 2013; Bastrikov et al., 2014). Based on a systematic investigation with different water standards, Weng et al. (2020) detected an additional dependency on the isotope ratio. While they proposed that this mixing ratio – isotope ratio dependency has a spectroscopic origin, they confirm that the shape of this measurement artefact is also specific for different instrument types and the used matrix gas (Aemisegger et al., 2012; Bailey et al., 2015).

https://doi.org/10.5194/amt-2023-55
Preprint. Discussion started: 17 April 2023

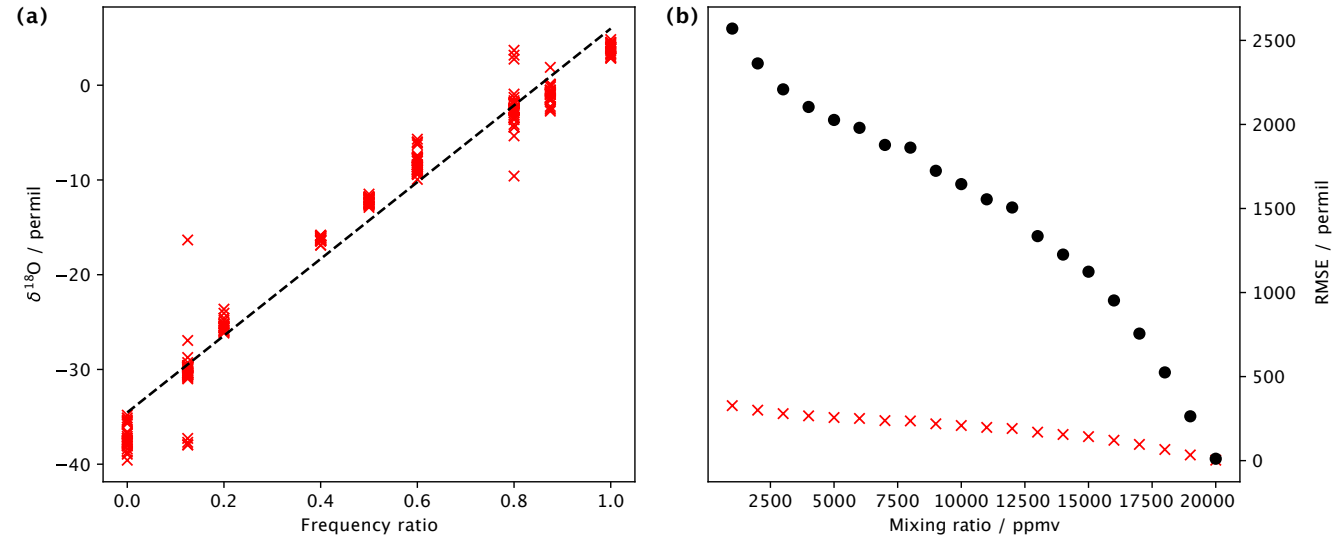

Figure 8. Stability of isotope standard mixing across range of humidities at an averaging time of 10 min. (a) Mixing line between two end members (laboratory standards DI2 and GLW) as a function of the ratio of dispensing frequency for δ^{18}O (‰) at different mixing ratios. Dashed black line is a 1:1 reference line. (b) Root-mean square error of the observed mixing line (‰), calculated using the reference line, as a function of different mixing ratios for δ^{18}O (red crosses) and δ^{2}H (black dots).

The correction procedure of Weng et al. (2020) allows to correct the uncalibrated isotope measurements for this artefact, in particular for low mixing ratios. However, two limitations have been identified in that study: (i) The characterization experiments with the above-mentioned vapour-generation techniques are time consuming, (ii) require manual preparation and calibration of additional standard waters, and (iii) are consequently based on a limited number of standards (5 in the case of Weng et al. (2020)). The microdrop calibration device presented here alleviates these difficulties by allowing to create an arbitrary mixture of standard waters at a specific isotope composition and mixing ratio, thereby providing the isotope composition–mixing ratio dependency for a given analyzer in high detail, specifically in regions of the mixing ratio – isotope ratio space where the artefact is particularly pronounced.

6.1 Experimental setup

The microdrop vapour generator was connected directly to the inlet of the Picarro analyser (L2130-i, Ser. No. HIDS 2254 or L2140-i, Ser. No. HKDS2038) with a stainless steel T-piece. Thereby, the overflow port was connected to the WLM Purge Port, secured by a check valve (Part Nr. SS-2C-1/3, Swagelok Inc, USA) to prevent leakage of ambient air into the analyzer inlet line. To achieve the desired humidity, the DH frequency was stepped up and down within a range of typically 1 to 100 Hz, while the flow rate of the dry matrix gas was set to 70, 100, 200 and 300 sccm.

https://doi.org/10.5194/amt-2023-55
Preprint. Discussion started: 17 April 2023

Atmospheric Measurement Techniques Discussions

Mixtures of the end member standards were injected by altering the DH frequency ratio for each of the two heads. For example, a 50 % contribution of enriched standard from DH1 (raw δ^{18}O=2.6 ‰ and δ^{2}H=12.1 ‰ at approximately 20000 ppmv) and 50 % of depleted standard (raw δ^{18}O=-39.7 ‰ and δ^{2}H=-311.9 ‰ at approximately 20000 ppmv) from DH2 would result in an intermediate raw mixed signal (raw δ^{18}O=-16.0 ‰ and δ^{2}H=-130.5‰ at approximately 20000 ppmv), taking into account the efficiency of the two DHs (see Sec. 4.2). The resulting mixture was named Mix50, given by the percent contribution of the enriched standard.

Each sequence typically covered a humidity range from about 20000 to 500 ppmv. An example for a typical humidity sequence during such a run (Fig. 9) shows the initial drying of the evaporation chamber to reach sufficiently low background mixing ratio (<100 ppmv) with N_2 prior each calibration sequence. Then, the gas supply was switched to the synthetic air, and the sequence starts by flushing the evaporation chamber with a vapour mix of standards specific for this sequence at a maximum frequency of 50 Hz for 5 min, followed by another drying to remove some vapour remaining from the previous run together with the new vapour. At the first calibration step, the frequency of 67 Hz was set for 6 s prior setting the desired 45 Hz at the DH1. This alternating pattern was used for quickly transitioning between two different humidity levels. Similarly, when stepping down from 45 to 39 Hz at the DH1, a 19 Hz frequency was used for a brief initial period from 13:55 to 13:56 (Fig. 9, before second step). The 60.0 s waiting time was set to adjust humidity before setting the desired frequency of 39 Hz. After the transitions, the frequencies were kept constant for 10 min, leading to plateaus of mixing ratio and isotope ratio. The transition period of 5 min between two concentrations was removed before further analysis. The precision during remaining periods (Fig. 9, red segments) was typically 8.2 ppmv (median of one-sigma standard deviation over a remaining 5 min period), with a range of 0.4 to 1722.3 ppmv.

6.2 Obtaining an isotope composition-mixing ratio dependency correction for a CRDS analyzer

To obtain the isotope composition-mixing ratio dependence functions for the same CRDS analyzer as in Weng et al. (2020) (L2130-i, Ser. No. HIDS2254), experiments with five different DH frequency ratios (100-80-60-40-20) covering the humidity range from 450 to 25000 ppmv have been conducted. Each experiment was repeated at least three times to obtain statistical significance of the measured results. Then, averages and standard deviation for each humidity step identified as above were calculated as described below. After an arbitrary stop of one of the DHs manual intervention was required. In some cases, leakage of water vapour from the second, stopped dispenser head required filtering for outliers. Here, measurement points for which the isotopic composition differs from the expected value at 20000 ppmv by more than 20 % have been excluded as outliers. Furthermore, the points for the mixing ratio above 5000 ppmv for which the standard deviation of the δ^{18}O-value exceeded the 75th quantile of the standard deviation of δ^{18}O for all measurements have been removed. These outliers occurred due strong variability in mixing ratio during the step or due to unstable functioning of one or both of the DHs, possibly due to formation of gas bubbles inside the DHs. The remaining data points, supplement by the measurements of Weng et al. (2020), were then used to construct the mixing ratio – isotope composition dependency correction (Fig. 10, blue points). As in previous studies, we use a reference value δ_{ref} at 20'000 ppmv to determine the deviation $\Delta\delta_{\text{corr}}$ of the raw isotope measurements from the reference value in untils of ‰ on a delta scale for mixing ratio x:

https://doi.org/10.5194/amt-2023-55
Preprint. Discussion started: 17 April 2023

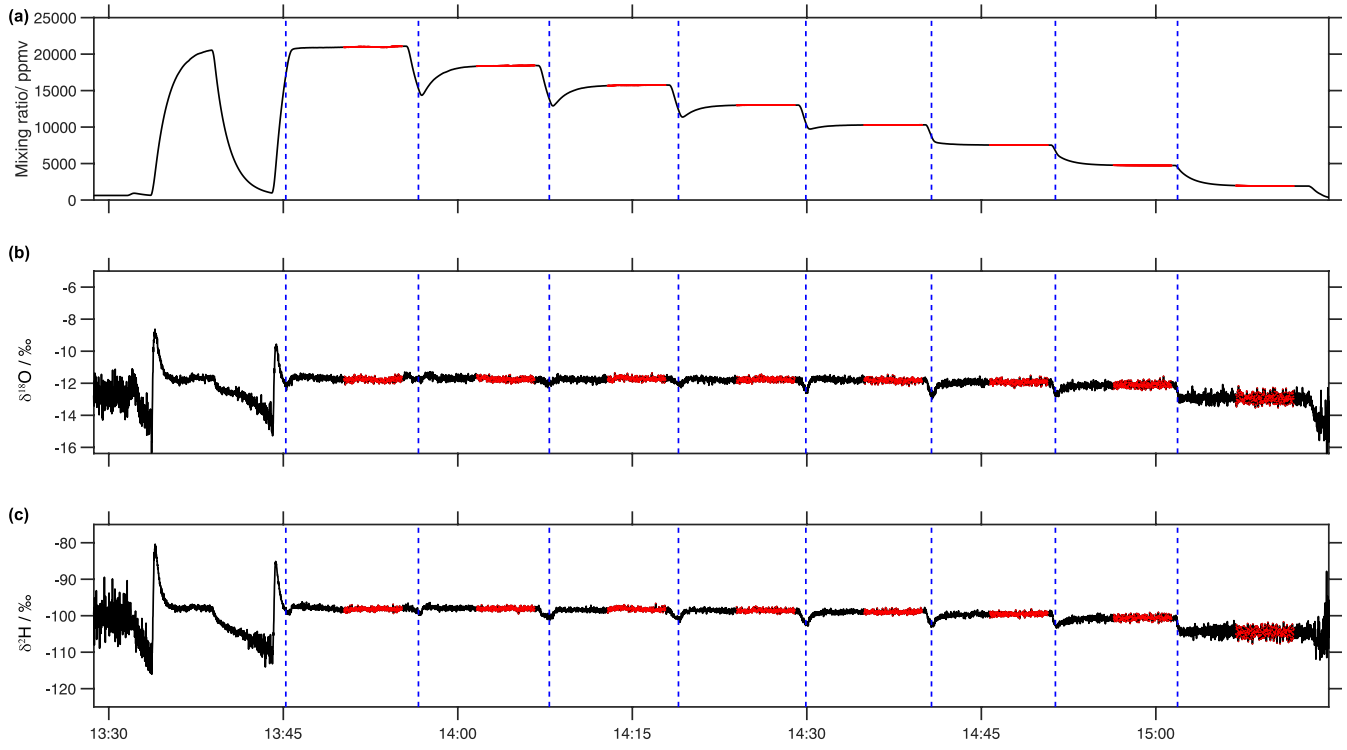

Figure 9. Typical sequence of (a) water vapour mixing ratio (ppmv), (b) δ^{18}O (‰) and (c) δ^{2}H (‰) during a calibration run on the FARLAB microdrop evaporator. Example depicts a run with Picarro analyzer HKDS2038 and synthetic air as a carrier gas, standard mixture Mix060 (60% DH1 and 40% DH2) on 04 June 2021, with 8 steps of 10 min duration (marked with dashed vertical blue lines) and 5 min stable period within each step (marked with red colour) used to calculate the average values and standard deviation of stable water isotopes and mixing ratio.

$$\Delta\delta_{\text{corr}}(\delta, x) = \delta(x) - \delta_{\text{ref}}. \tag{2}$$

While Weng et al. (2020) used hyperbolic functions of mixing ratio fitted to measurement points with a set of water standards, we use a new approach that is more flexible in terms of utilizing data points that are mixed from different waters by the microdrop device. To this end, we first remove the dominant first-order dependency on the mixing ratio by a log-transformation of the mixing ratio to $\ln(x)$:

$$\Delta\delta_{\text{corr}}(\delta, \ln(x)) = \delta(\ln(x)) - \delta_{\text{ref}}. \tag{3}$$

To take all measurements into account, we obtain the reference value δ_{ref} from a 2nd-order polynomial fit to each measurement sequence at a specified isotope ratio. Next, we fit a regular second or third order two-dimensional polynomial to the set of

https://doi.org/10.5194/amt-2023-55
Preprint. Discussion started: 17 April 2023

Atmospheric Measurement Techniques Discussions

Table 3. Difference between data points obtained from micodrop measurements and different mixing ratio – isotope ratio correction surfaces, quantified as root-mean square error (RMSE).

RMSE	δD	δ^{18}O
Weng et al. (2020)	1.6630	0.2276
polynomial fit	0.7009	0.1780
polynomial fit with zero adjustment for reference mixing ratio	0.8184	0.2305

deviations. We find that different analyzers require different polynomials for fitting in the $\Delta\delta$ and the $\ln(x)$ direction. For the four analyzers investigated at FARLAB, a 2nd-order polynomial was sufficient along the $\ln(x)$ axis. Two of the four analyzers had better fitting results with a 3rd-order polynomial in the $\Delta\delta$ direction than with a 2nd-order polynomial. An example for analyzer HIDS2254 shows that the surfaces are to a large degree consistent with the measurement data (Fig. 10).

As a final processing step, to avoid false corrections at reference humidity, we subtract the deviation from zero of the fitted surface at reference humidity along each isotope ratio. Thereby, the RMSE of the correction surface in comparison to the measurement points increases (Table 3). For δ^2H, the RMSE increase is smaller than for δ^{18}O, where the RMSE is very similar to the correction surface of Weng et al. (2020). Despite the different approach compared to Weng et al. (2020), the shape of the correction surface is to first order remarkably consistent with previously published results for the same analyzer (Fig. 11a,b; black and blue lines). Compared to measurements, the root-mean square error of the correction obtained in this study is 0.82 ‰ for δ^2H and 0.23 ‰ for δ^{18}O with adjustment for zero at reference mixing ratio (Table 3).

Due to the mixing capability of the microdrop device, it is possible to make additional measurements in-between available laboratory standards, and without mixing additional waters beforehand. We also extended the range of the correction to between 5 and -40 ‰ for δ^{18}O and to 10 and -350 ‰ for δ^2H using additional secondary standards. Notably, the microdrop device allows to obtain the data points needed for such a correction function in a semi-automated fashion and with large flexibility. For example, based on this first screening of the dependency for this analyzer, it would be possible to zoom into particularly critical regions og a given analyzer's dependency function, such as the region with mixing ratios below 2000 ppmv in the δ^{18}O dependency for the current device (Fig. 11b, red shading).

The surface fitting approach presented here also allows to quantify the uncertainty of the surface fits, thus providing access to the contribution from the mixing ratio – isotope ratio correction to the total uncertainty of a final data set. Here, we used a Monte-Carlo approach to determine the standard deviation of the correction values from 50 realisations of a sub-sample of all available measurements. Standard deviations are largest at the edges of the correction surface, with values of up to 0.6 ‰ for δ^2H (Fig. 11c) and 0.2 ‰ for δ^{18}O (Fig. 11d). Near the center of the correction functions, the uncertainty is much smaller than the correction itself, as constrained by the precision of the sub-sampled microdrop-generated dataset.

https://doi.org/10.5194/amt-2023-55
Preprint. Discussion started: 17 April 2023

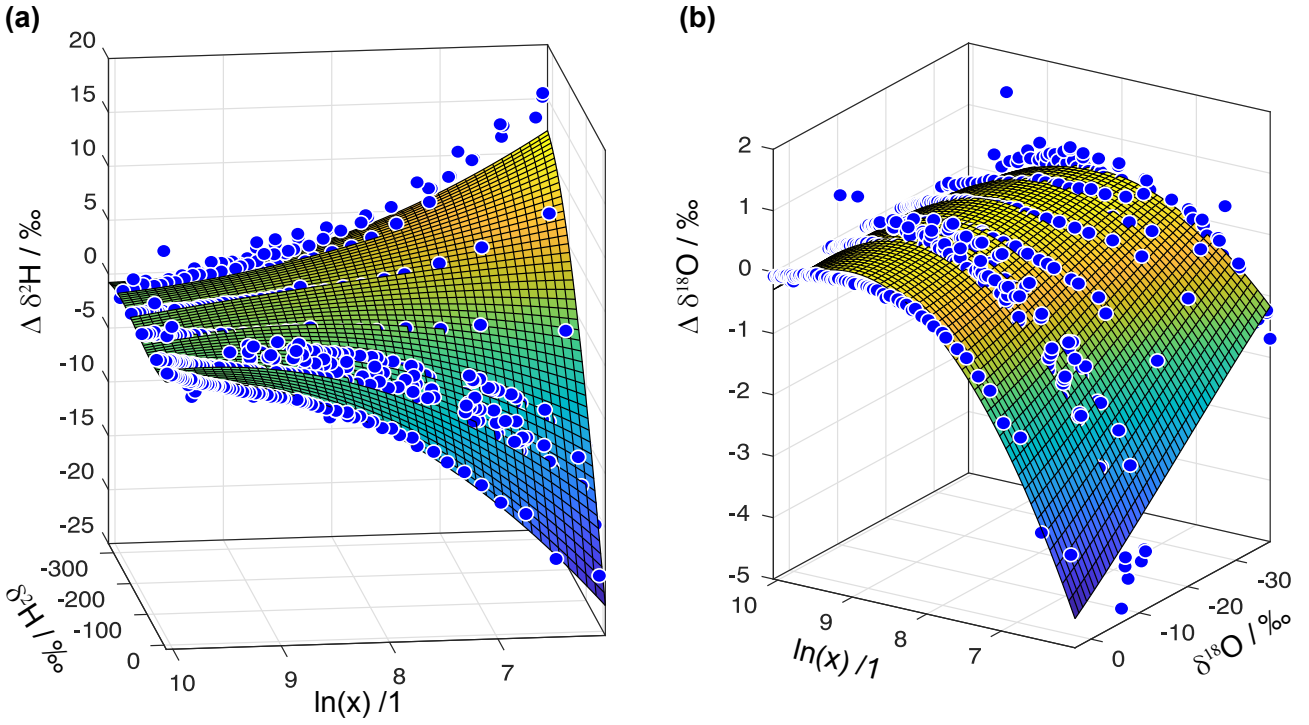

Figure 10. Surface fitting for instrument HIDS2254 for (a) δ^2H and (b) δ^{18}O as a function of ln(mixing ratio). Blue dots show measurement points obtained from microdrop device to constrain the surface fit.

7 Application 2: δ^{18}O and δ^2H values of fluid inclusions in stalagmites

We now present an example for an analytical set-up in the laboratory where the microdrop device produces a constant vapour stream for fluid inclusion analysis from stalagmites. Voids within the carbonate matrix of stalagmites regularly preserve remnants of cave drip waters. Since these waters are the relics of past precipitation, their oxygen and hydrogen isotope compositions can be used to reconstruct past changes in cave temperature (e.g., McGarry et al., 2004; Meckler et al., 2015) and changes in the amount and/or source of precipitation (Fleitmann et al., 2003). Due to the small size of inclusions (<100 μm) and the low amount of water that is commonly present in stalagmites (0.05 to 0.5 weight%; Affolter et al. (2014)), isotope measurements are made on the water that is released when large aliquots (>50 mg) of carbonate are crushed in a heated apparatus. Due to the small water amounts, analysis of fluid inclusions in stalagmites requires a background vapour stream with precisely known isotope composition and mixing ratio as carrier gas. This known background enables to separate the superimposed δ^{18}O and δ^2H signals of the water released from calcite cavities during the crushing.

Measurements have traditionally been obtained with isotope ratio mass spectrometers (IRMS), but these tend to be slow and cumbersome partly due to large memory effects that must be accounted for (e.g., de Graaf et al., 2020). Recent work, however,

https://doi.org/10.5194/amt-2023-55
Preprint. Discussion started: 17 April 2023

Atmospheric Measurement Techniques Discussions

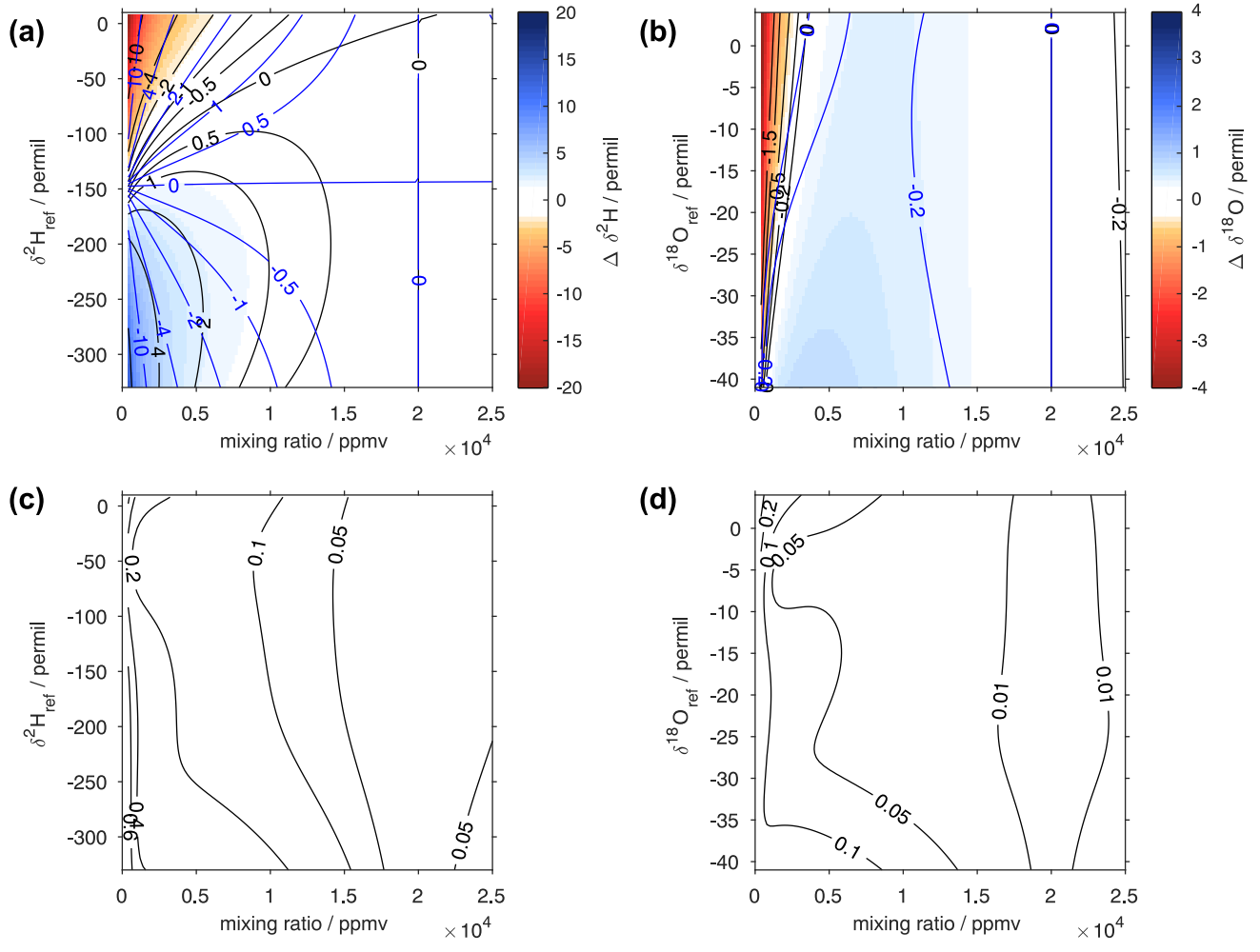

Figure 11. Surface function of the isotopic deviations for (a) δ^{18}O and (b) δ^{2}H based on the isotope composition–mixing ratio dependency of Picarro analyzer HIDS2254 (Picarro L2130-i). The horizontal axis is the raw mixing ratio, and the vertical axis shows the raw isotope composition at 20'000 ppmv. Contours with numbers indicate the isotopic deviation of $\Delta\delta$. Dashed grey lines show the correction functions of Weng et al. (2020). Lower row: standard deviation of correction function obtained from a Monte-Carlo Approach for (c) δ^{2}H and (d) δ^{18}O (‰) using 50 random sub-sets of the entire dataset.

has demonstrated that memory effects can be removed entirely with CDRS techniques if analytical devices (stainless steel lines and crusher devices) are kept under humid conditions (Affolter et al., 2014). Fluid inclusion waters are then measured on top of a constant background, which is subtracted after peak integration. The result is higher sample throughputs and better reproducibilities (Affolter et al., 2014; Dassié et al., 2018; de Graaf et al., 2020). Here we describe how the micro-dropper

https://doi.org/10.5194/amt-2023-55
Preprint. Discussion started: 17 April 2023


Atmospheric Measurement Techniques Discussions

device is able to produce a water background of constant isotopic compositions that can be used to obtain accurate and precise fluid inclusion δ^{18}O and δ^{2}H measurements.

7.1 Measurement and data reduction procedures

An analytical line for the sample crushing device (crusher) was built from stainless steel following the design described by Affolter et al. (2014) and de Graaf et al. (2020) (Fig. 12). The upper end is connected to the microdrop device, and the downstream end is connected directly to the analyzer HIDS2254 (L2130-i, Picarro Inc) with a union tee fitted with a 1/16 inch capillary as open split. A check valve (Part No. SS-2C-1/3, Swagelok Inc., USA) was installed before the injection port to prevent backflow of sample waters. The injection port consists of a union tee fitted with a rubber septum. The last component is a particle filter (7 μm, Part No. SS-2F-7, Swagelok Inc., USA), which was installed to prevent sample powder from reaching the analyzer. All parts of the line are heated to 120 °C with the use of an oven (FP 53, Binder GmbH, Germany) or silicon rubber heating tapes (EHG series, Watlow, USA). The crusher is made entirely of stainless steel and it is based on the design by de Graaf et al. (2020) with some modifications (Fig. A2). Two Viton O-rings are used to seal the device from atmospheric gases. One ring is placed on top of the base, and the other is placed on the piston. The piston is threaded to allow up and down movements.

Before an analytical session, the N_2 flow into the microdrop device is set to 90 sscm, the excess above the 35 sccm used by the analyzer is vented through the open split. The DH is then set to deliver the number of drops per second needed to produce a constant mixing ratio of typically 10'000 – 15'000 ppmv for frequencies of 60-120 Hz. A sample is subsequently loaded into the crusher, and a period of about 20 min is needed for the background H_2O mixing ratio and δ^{18}O and δ^{2}H values to stabilize (Fig. 13, grey area). Once the background is stable, the oven is opened and the thread of the crusher is turned to pulverize the sample, which causes the fluid inclusions waters to evaporate instantaneously. Typically, about 10-12 min are needed to measure a complete sample peak.

After the water is measured by the analyzer, the data is processed with a series of MATLAB scripts that: (i) correct δ^{18}O and δ^{2}H values for their humidity dependence (see Sec. 6), (ii) integrate peaks and subtract background values, and (iii) normalize δ^{18}O and δ^{2}H values to the VSMOW scale and calculate sample H_2O concentrations with standards of known compositions. Mixing ratio – isotope ratio corrections are performed as described in Sec. 6. This is an important step, as the magnitude of the correction depends both on the size of a sample (i.e., amount of water released) and its isotopic composition (Fig. 11). These corrections have not been previously performed in fluid inclusion CDRS data, which may explain why some laboratories observe a size-δ relationship that varies for different standards (e.g., de Graaf et al., 2020).

The next step in the data reduction procedure is to integrate the area under the sample peaks and subtract the background. This was done following the algorithms described in Affolter et al. (2014). Briefly, raw isotope and H_2O ppmv data (peak and background) are first passed through a running mean filter with a 10 s window to smooth out high frequency variability. The algorithm then finds the start of the peak, which is defined when the rate of change in the water concentration exceeds 5.5 ppmv s^{-1}. Since the rate quickly increases and then turns negative at the top of the peak, the end of the peak is defined after the rate returns to positive values. Next, background values are calculated by averaging values before and after the peak; this was done

https://doi.org/10.5194/amt-2023-55
Preprint. Discussion started: 17 April 2023

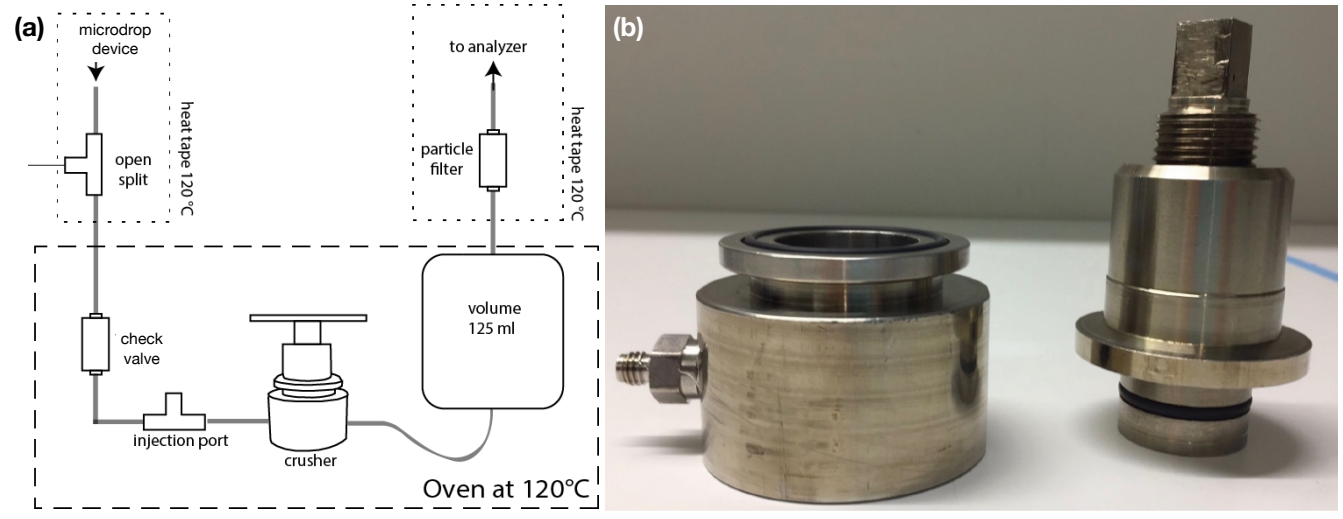

Figure 12. Setup of the crusher system. (a) Schematic of the analytical line for the crusher system. (b) Photograph of the crusher device, built after de Graaf et al. (2020).

to account for possible drift in values. After background subtraction, raw sample δ^{18}O and δ^{2}H values were normalized to the VSMOW scale with three different in-house standards, which were previously calibrated against international standards. For calibration, a range of water amounts (0.05 to $\sim$1.5 μl) were injected with the aid of autosampler GC syringes (0.5 μl SGE Analytical Science and 1 μl Thermo Scientific), and their mean values were used to build a transfer function (Fig. A1). While this step may appear redundant (Sec. 6), it ensures that samples and standards receive identical treatments, in particular as the crusher device with calcite remnants and the particle filter can induce different humidity dependencies. Finally, the amount of water released by the samples was obtained from a transfer function constructed with the calculated amounts of water of a series of different samples and the known amounts that were injected.

7.2 Data accuracy and reproducibility

To estimate the reproducibility of our analyses we calculated pooled standard deviations every 0.1 μl (Fig. A2). This was done with the injections used for scale normalization. We observe that standard deviations are very similar for samples larger than 0.3 μl ($<$0.3‰ for δ^{18}O and $<$1.3 ‰ for δ^{2}H), increase for smaller samples, and are the largest for samples smaller than 0.1 μl (0.7‰ for δ^{18}O and 3.4 ‰ for δ^{2}H). These reproducibilities are in the range of what has been observed in similar set-ups (Affolter et al., 2014; Dassié et al., 2018; de Graaf et al., 2020).

As a final test of data quality, we measured two samples that have known isotopic compositions. One of the samples consists of 24 aliquots of 0.2 to 0.6 μl of DI standard water that were sealed in borosilicate glass capillaries and crushed in the analytical line (Fig. 14c). Replicates of this sample are designed to mimic real fluid inclusions since, unlike injections, they receive the

https://doi.org/10.5194/amt-2023-55
Preprint. Discussion started: 17 April 2023


Atmospheric Measurement Techniques Discussions

same treatment (i.e., water is released in the same location by turning the thread of the crusher device; Weissbach (2020)). We find that the mean value of these analyses (δ^{18}O=-7.5$\pm$0.3‰ and δ^{2}H=-50.9$\pm$1.2‰; $\pm1\sigma$) are statistically indistinguishable from their 'known' values (Fig. 14a). The second sample (Fig. 14b) is an aliquot of a natural carbonate (Semproniano travertine) that has been previously measured in another laboratory. A total of 4 aliquots of this sample were analyzed, and their mean values (δ^{18}O=-4.3$\pm$0.3‰ and δ^{2}H= -34.3$\pm$1.7‰;$\pm1\sigma$) are statistically indistinguishable from the results obtained by de Graaf et al. (2020) (δ^{18}O=-4.6$\pm$0.32‰ and δ^{2}H= -33.4$\pm$0.9‰; $\pm1\sigma$, n=4).

In summary, the microdrop vapour generation device enabled a two-fold improvement of the application setup for the measurement of fluid inclusions. First, the characterisation of the analyzer allows to correct for the mixing ratio – isotope ratio dependency of the analyzer signal, providing a more correct integrated signal of each sample. With the variable water amounts and isotope composition in each sample, this appears as an important additional processing step. Second, the precise background signal of the microdrop device with short-term variance of $\sim$10 ppmv on the time scale of the handling of the crushing device provides a noise-free environment to separate the signal of the fluid inclusion water reliably from the background water stream. In combination, both aspects demonstrate the value of the microdrop technology for specific water isotope measurement applications.

8 Critical operational aspects and potential error sources

During the operation procedure (Sec. 4), and during operation of one of the application examples (Sec. 6), a number of problems may occur that interrupt or disturb experiments. While in general working reliably over several hours at a time, these problems are important to be aware of, and one needs to search for remedies in future development of the calibration system.

Finding suitable parameters for single droplet formation, rather than a jet of droplets, is cumbersome and time-consuming process, but should be a rarely repeated procedure for each DH that is utilized. Potential problems ensue from undetected jets of droplets, that can lead to non-linear or noisy DH characteristics (Sec. 4.2).

During droplet generation, several problems and interruptions can occur. Sturm and Knohl (2010) already reported that the droplet generation stopped occasionally, probably due to formation of bubbles in the injector as the liquid warms up. The procedure involving an ultrasonic bath (Sec. 4.4, step 2) is intended to prevent such bubbles from forming. A further cause for stopping droplet generation can be clogging due to fine particles or residue of salts building up at the dispenser head. While salts can be removed by cleaning procedures, a clogged dispenser head may have to be replaced at some point. Filtering of the standard liquid (Sec. 4.4, step 1) is therefore imperative. While it is conceivable that direct evaporation from the DH capillary may occur at high temperatures and low frequencies, thereby stopping DH operation, more evidence is needed to confirm this potential error source. A final parameter that could influence DH operation is the holding pressure. The holding pressure is a slight underpressure created by the microdrop controller in the standard vials to prevent liquid from running freely into the evaporation chamber. While typically a holding pressure of about -10 Pa was employed, it could be worth exploring dispensing behaviour for lower holding pressure, in particularly for horizontally mounted DHs.

https://doi.org/10.5194/amt-2023-55
Preprint. Discussion started: 17 April 2023

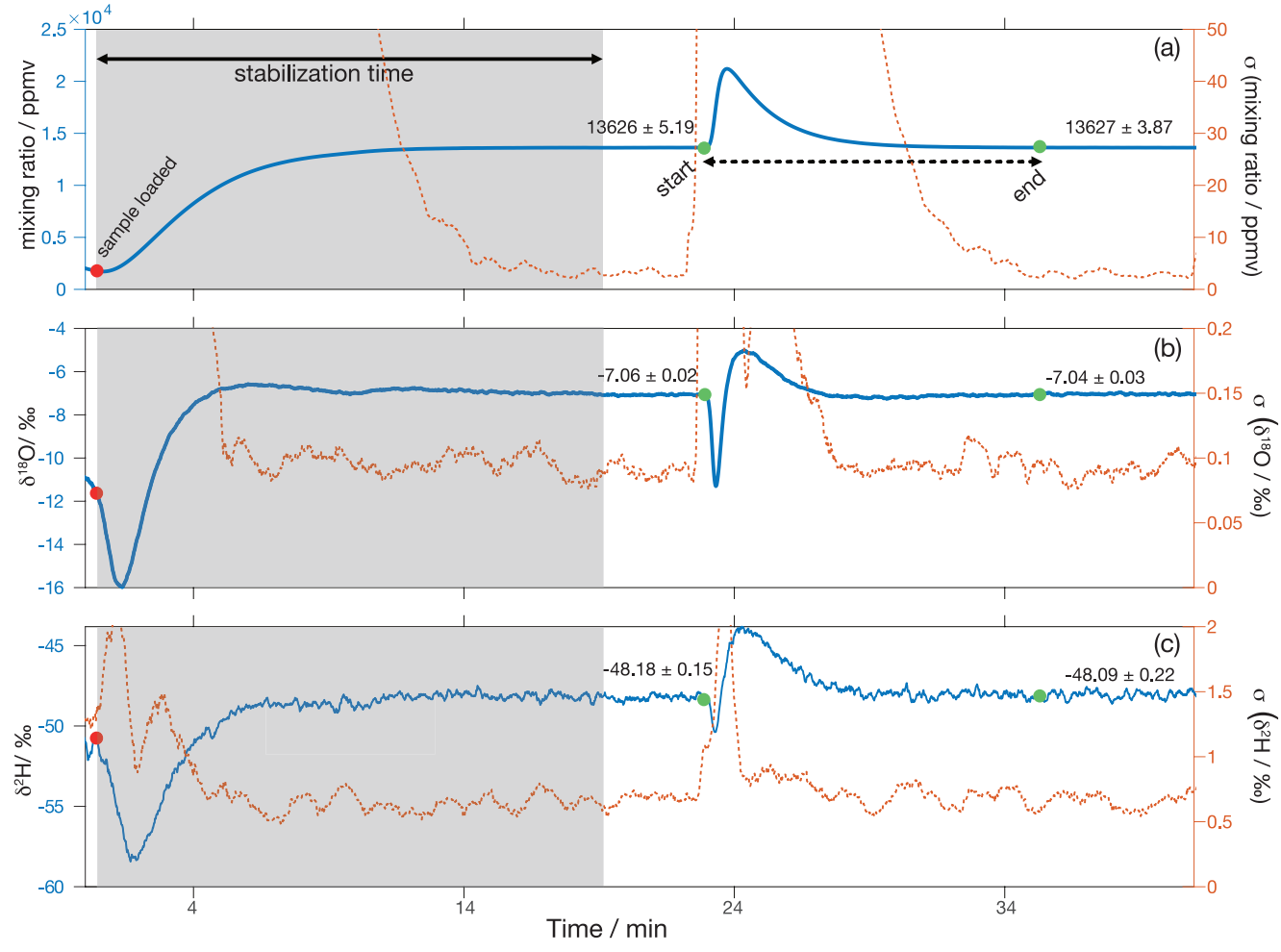

Figure 13. Example of a typical analysis with the crusher and microdrop device. Approximately 18-20 minutes are needed for (a) mixing ratio, and the two water isotope species (b) δ^{18}O and (c) δ^{2}H to stabilize after a sample has been loaded into the crusher device (red circle, ∼1 minute). The left axis shows average raw measurements acquired at 0.9 Hz filtered through a 30 s running mean filter, and the right axis shows the standard deviations of the running mean. Background average values before and after the peaks are shown in all panels. Peak values are integrated between the green markers, which show the start and the end of the peak.

During operation of both dispenser heads, the discrete frequency settings for each DH cause limitations of the mixing ratios between both standard liquids. For example, if both DHs are to contribute no more than 5 drops per second in total, obtaining a partitioning of 1:2 between both heads would require non-integer trigger frequencies, which are currently not allowed by the microdrop controller software. To circumvent this problem, the calibration system can be operated at higher gas flow rates and corresponding higher frequencies.

https://doi.org/10.5194/amt-2023-55
Preprint. Discussion started: 17 April 2023

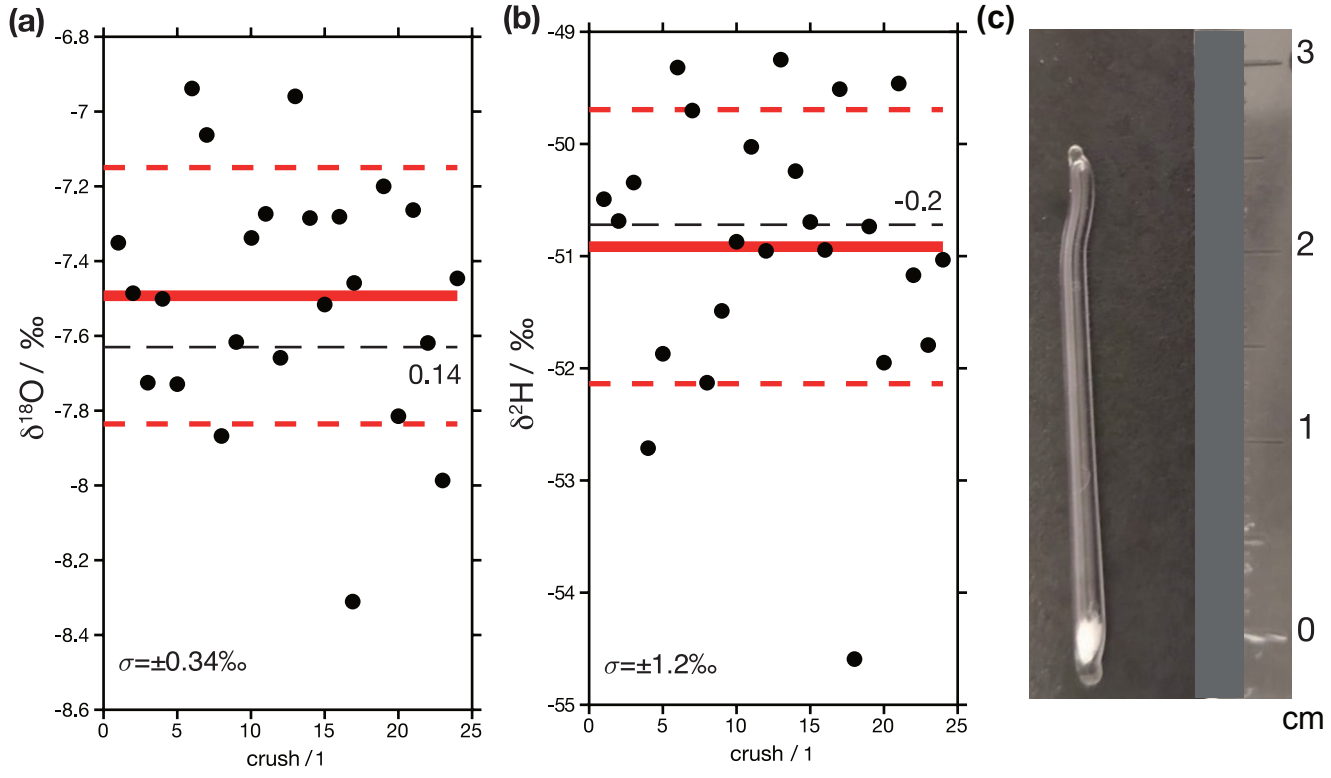

Figure 14. Results from crushed glass capillaries loaded with DI standard. (a) δ^{18}O values. The red line shows the mean value of the replicates, and the dashed red lines are the ± 1 standard deviation. The black dashed line is the 'true' value of the standard, which is 0.14‰ lower than measured mean value. (b) δ^{2}H values. In this case the 'true' value of the standard is 0.2 ‰ higher than the measured mean value. (c) Photograph of a loaded glass capillary. These are built from the capillaries of borosilicate glass pipets. The bottom is sealed and loaded with quartz wool, and water is injected into the wool. The top of the pipet is then sealed.

If the calibration system is connected to a downstream application that requires a similar amount of gas flow as the calibration system provides (e.g., a CRDS analyzer operating in high-flow mode), ambient air may enter the analyzer and create an offset in isotope ratio and mixing ratio of the calibration air stream. There are additional aspects that are worth to investigate further, such as the change of viscousity of the water due to heating in the cavity, and the build-up of overpressure in the evaporation chamber at larger flow rates. With active control of such parameters, it can be expected to further increase the precision of the device across a range of flow rates.

https://doi.org/10.5194/amt-2023-55
Preprint. Discussion started: 17 April 2023


Atmospheric Measurement Techniques Discussions

9 Conclusions and implications

Here we describe a new device for the generation of a vapour stream of a specified mixing ratio and water isotope composition. The device is based on microdrop dispensing, adding to the few previous designs of vapour generators for isotope applications with this technology. As a key innovation, we operate two dispenser heads in parallel to enable creating a vapour stream with any value along a mixing line between two water standards. We characterize the microdrop vapour generator in terms of the precision of the vapour stream mixing ratio and isotope composition on long and short time scales. Short-term uncertainty of the vapour stream, quantified as Allan deviation, is on the order of for 5–10 ppmv for H_2O, about 0.03 ‰ for $\delta^{18}O$ and about 0.2 ‰ for $\delta^{2}H$ for averaging times of up to 30 s. These values are substantially better than a comparable set of measurements obtained with the SDM. The long-term precision of 15 min measurement intervals is on the order of 10 ppmv for H_2O, 0.10 ‰ for $\delta^{18}O$, and 0.65 ‰ for $\delta^{2}H$. These estimates are not substantially affected by either flow rate or dispensing frequency. Simultaneous operation of two dispenser heads provides a linear mixing between two standard waters. The general characteristics of the design in terms of response to flow rate and simultaneous operation of the dispenser heads thus demonstrate that the device functions overall according to specifications.

We use the microdrop vapour generator in two application settings. First, we obtain a semi-automated characterisation of the mixing ratio – isotope ratio dependency for an analyzer in a wide range, more precisely, and with lower effort than previously possible. Using a simplified fitting procedure, we obtain a 2-dimensional correction function. The correction function shows similar overall shape and characteristics for the same analyzer over time as in Weng et al. (2020), confirming the stability of this analyzer characteristic over months to years. In a second application, we use the microdrop vapour generator in an analytical setup with a crusher device for the analysis of fluid inclusion isotope composition of stalagmite samples. Analysis of standard sample material confirms that the overall analysis works correctly. The high precision of the background humidity from the microdrop vapour generator is a valuable asset in obtaining precise results from the crusher line. Importantly, the availability of a mixing ratio – isotope ratio characterisation for the analyzer enables correction of this analyzer artefact during peak integration, a factor which has been neglected in previous fluid inclusion studies.

The main advantages of the design are, besides the high precision of the signal, its flexibility in terms of mixing ratio and isotope ratio, absence of moving parts, and low power consumption. Challenges are the occasional stopping of the dispenser head that requires manual intervention, and the startup procedure. In addition to a higher degree of automated operation, transfer to a more robust, field-deployable design would clearly be an advantage over the current prototype version. Nonetheless, our successful demonstration of the overall design has several implications for the water vapour isotope measurements:

The availability of a source of standard vapour that works at different flow rates, mixing ratios, and stable isotope ratios will offer a range of possible applications, from regular calibration and instrument or inlet system characterisation, to more specialized operations, involving external equipment. With the availability of a precise vapour generator, commercial CRDS analyzers can be more commonly corrected for measurement artifacs such as the mixing ratio – isotope ratio dependency. In addition to analyzer characteristics, the inlet system can influence the measurement signal due to interaction with walls, manifolds, and filters. Tubing to guide ambient vapour to a CRDS analyzer can affect the isotope composition through memory

https://doi.org/10.5194/amt-2023-55
Preprint. Discussion started: 17 April 2023


Atmospheric Measurement Techniques Discussions

effects, that result differential retention times at the tubing walls. These effects are dependent on both material, surface structure, and coatings. Prominently, Synflex tubing has been shown to render δ^2H measurements meaningless. Different materials response time to either humidity or isotope composition switches require a stable and well-characterized vapour source. Such effects can be identified and characterised by the provision of known pulses of water vapour and water isotopes onto the inlet system. As a result, signals can either be corrected, or averaged in a suitable way to allow a more reliable separation between geophysical and instrumental signals than is currently possible.

Code and data availability. The data set and program code are available from the authors on request.

Appendix A: Crusher application details

https://doi.org/10.5194/amt-2023-55
Preprint. Discussion started: 17 April 2023

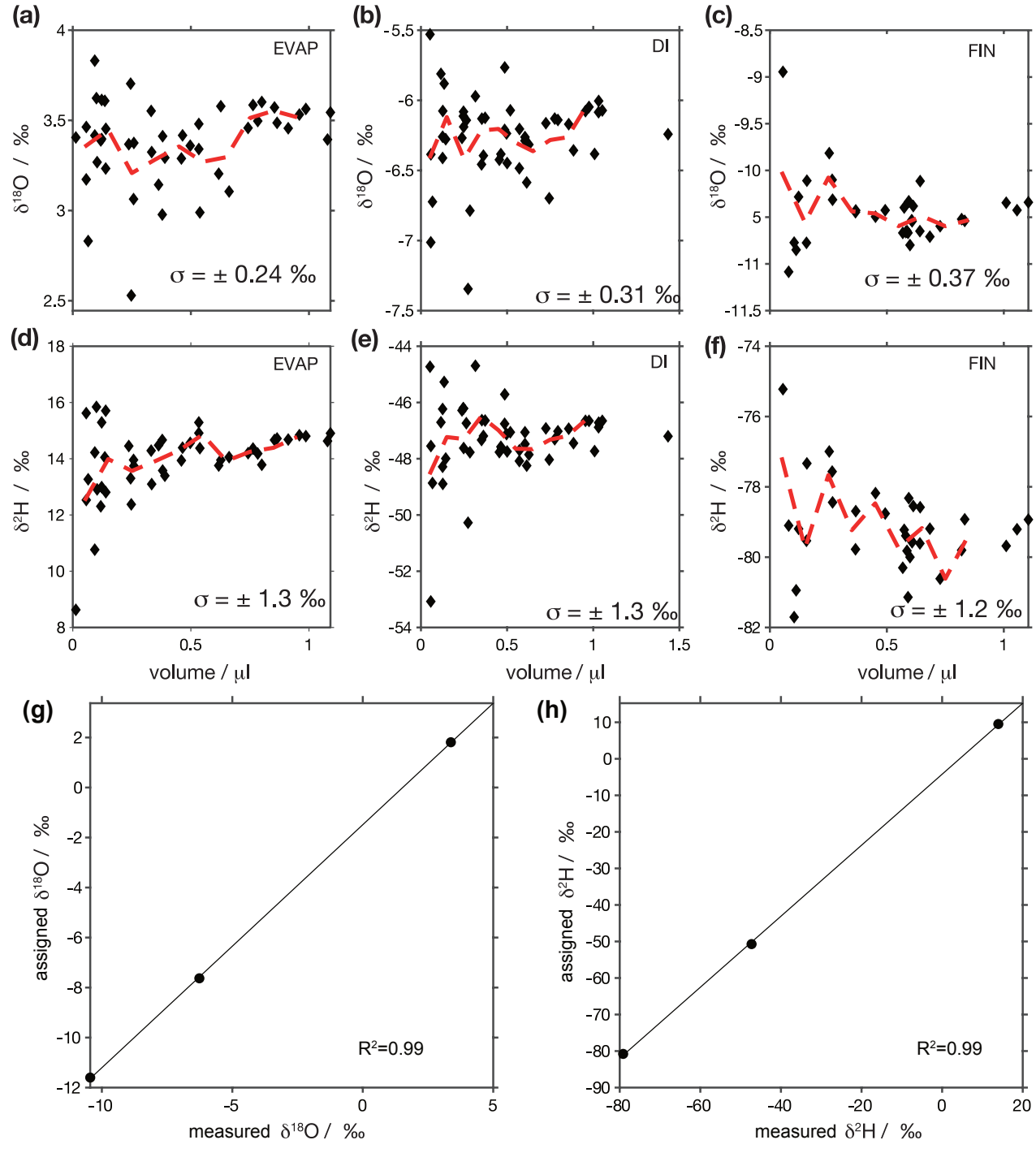

Figure A1. Sample waters are calibrated with three inhouse standards (previously normalized to VSMOW-SLAP). Panels (a-f) show $\delta^{18}O$ and $\delta^{2}H$ values for injections of different volumes. Red dashed line are the mean values of the standards averaged every 0.1 μl. Panels (g) and (h) show transfer functions constructed from panels a-f with the mean measured vs. assigned values for $\delta^{18}O$ and $\delta^{2}H$.

https://doi.org/10.5194/amt-2023-55
Preprint. Discussion started: 17 April 2023

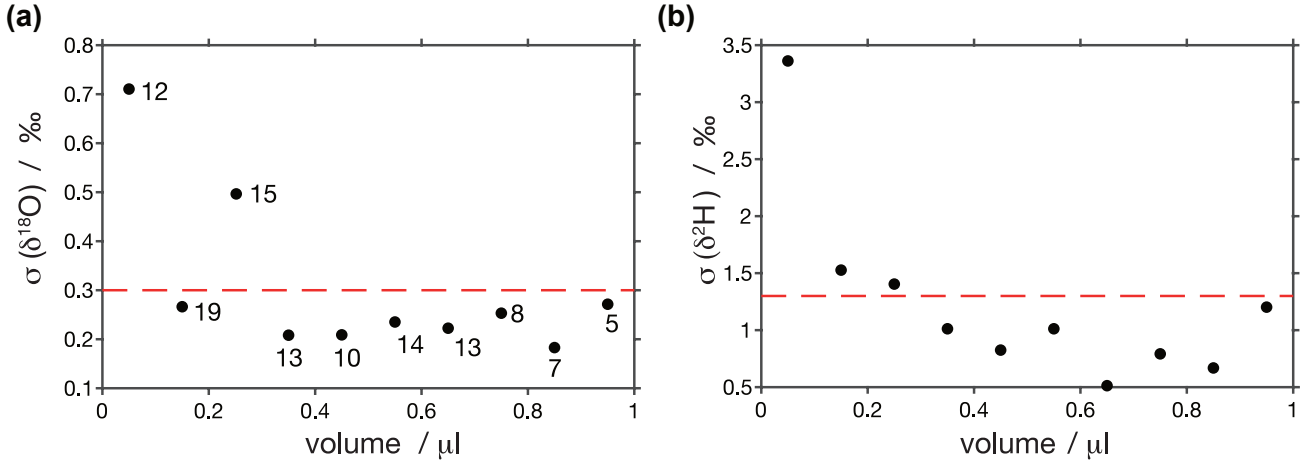

Figure A2. Pooled variance of injections calculated every 0.1 μl. Reproducibilities for samples larger than 0.3 μl are <0.3‰ for (a) δ^{18}O and <1.3 ‰ for (b) δ^{2}H and increase for smaller samples. Circles are labelled with number of injections used to calculate pooled variance at each point.

https://doi.org/10.5194/amt-2023-55
Preprint. Discussion started: 17 April 2023

Atmospheric Measurement Techniques Discussions

Table A1. Date, time, and mixing ratio of the 37 segments used for the short-term stability assessment. Time is the begining of the 15 min interval used to calculate standard deviations in water background and isotope values.

Date	Time	Mean(H_2O)	SD(H_2O)	SD($\delta^{18}O$)	SD($\delta^{2}H$)
2020-10-02	12:51:07	11524	29.8	0.133	0.661
2020-10-06	17:02:47	11266	13.6	0.114	0.668
2020-10-09	12:27:45	11193	26.6	0.135	0.673
2020-10-11	15:39:44	11154	10.5	0.098	0.618
2020-10-14	10:51:25	11456	10.6	0.099	0.648
2020-10-14	13:00:50	11444	4.2	0.097	0.647
2020-10-14	14:37:03	11478	4.6	0.091	0.633
2020-10-19	10:14:18	9608	10.3	0.099	0.632
2020-10-19	12:18:44	9558	5.8	0.099	0.630
2020-10-19	13:01:35	9561	3.9	0.097	0.627
2020-10-20	10:37:04	11672	6.5	0.100	0.671
2020-10-20	12:23:13	11640	14.0	0.102	0.662
2020-10-22	13:03:44	12026	10.1	0.096	0.655
2020-10-22	14:30:00	12050	13.1	0.098	0.642
2020-10-23	11:18:42	12079	7.3	0.095	0.644
2020-10-23	12:36:16	12080	9.1	0.097	0.644
2020-10-23	13:44:41	12060	8.5	0.101	0.641
2020-10-27	13:29:00	12064	11.6	0.098	0.653
2020-10-27	17:46:53	12208	8.8	0.099	0.665
2020-10-28	10:19:02	12170	9.7	0.094	0.602
2020-10-28	11:36:25	12092	12.7	0.099	0.644
2020-10-28	14:30:23	11981	10.0	0.102	0.640
2020-10-28	15:28:51	11901	11.8	0.105	0.640
2020-10-30	11:34:02	12286	18.5	0.118	0.661
2020-11-02	11:09:05	12327	11.9	0.098	0.646
2020-11-02	13:57:04	11937	17.9	0.108	0.659
2020-11-02	15:25:24	11928	23.2	0.124	0.668
2020-11-03	11:31:10	11887	24.4	0.130	0.687
2020-11-03	12:09:20	12006	21.8	0.107	0.672
2020-11-06	16:45:40	13346	5.7	0.095	0.674
2020-11-06	17:41:55	13360	6.8	0.099	0.638
2020-11-10	11:52:19	13425	12.5	0.096	0.647
2020-11-10	12:55:17	13390	4.2	0.096	0.643
2020-11-10	17:51:03	13116	6.3	0.092	0.636
2020-11-11	16:40:10	13151	6.7	0.095	0.643
2020-11-11	18:24:41	13053	5.5	0.099	0.674
2020-11-11	19:23:35	13019	8.5	0.098	0.662

https://doi.org/10.5194/amt-2023-55
Preprint. Discussion started: 17 April 2023

Atmospheric Measurement Techniques Discussions

Author contributions. HS designed and built the microdrop device and contributed to experiments, data analysis, and writing. AD perfomed experiments for analyzer characterisation, data analysis, and writing. AFB built the crusher application, performed experiments and data analysis, and contributed to the writing. AS contributed to data analysis and visualisation. JM contributed to experiments, data analysis and interpretation. All authors contributed to the revision of the final submitted manuscript.

Competing interests. The authors declare no competing interests.

Acknowledgements. The authors acknowledge FARLAB, University of Bergen, Norway for provision of analyzers and laboratory space. Enver Alagoz is acknowledged for help with the thermal regulation of the microdrop device. We thank Microdrop GmbH for support regarding the software control of the dispensing heads. AF acknowledges support from Juan de la Cierva Fellowship (IJC2019040065-I) granted by the Spanish Ministry of Science and Innovation and co-funded by the European Development Fund and the European Social Fund.

https://doi.org/10.5194/amt-2023-55
Preprint. Discussion started: 17 April 2023

Atmospheric Measurement Techniques Discussions

References

Aemisegger, F., Sturm, P., Graf, P., Sodemann, H., Pfahl, S., Knohl, A., and Wernli, H.: Measuring variations of δ¹⁸O and δ²H in atmospheric water vapour using two commercial laser-based spectrometers: an instrument characterisation study, Atmospheric Measurement Techniques, 5, 1491–1511, 2012.

Affolter, S., Fleitmann, D., and Leuenberger, M.: New online method for water isotope analysis of speleothem fluid inclusions using laser absorption spectroscopy (WS-CRDS), Climate of the Past, 10, 1291–1304, 2014.

Bailey, A., Noone, D., Berkelhammer, M., Steen-Larsen, H. C., and Sato, P.: The stability and calibration of water vapor isotope ratio measurements during long-term deployments, Atmospheric Measurement Techniques, 8, 4521–4538, 2015.

Bastrikov, V., Steen-Larsen, H. C., Masson-Delmotte, V., Gribanov, K., Cattani, O., Jouzel, J., and Zakharov, V.: Continuous measurements of atmospheric water vapour isotopes in western Siberia (Kourovka), Atmospheric Measurement Techniques, 7, 1763–1776, 2014.

Bonne, J. L., Masson-Delmotte, V., Cattani, O., Delmotte, M., Risi, C., Sodemann, H., and Steen-Larsen, H. C.: The isotopic composition of water vapour and precipitation in Ivittuut, southern Greenland, Atmospheric Chemistry and Physics, 14, 4419–4439, 2014.

Bonne, J.-L., Behrens, M., Meyer, H., Kipfstuhl, S., Rabe, B., Schönicke, L., Steen-Larsen, H. C., and Werner, M.: Resolving the controls of water vapour isotopes in the Atlantic sector, Nature Communications, pp. 1–10, 2019.

Dassié, E. P., Genty, D., Noret, A., Mangenot, X., Massault, M., Lebas, N., Duhamel, M., Bonifacie, M., Gasparrini, M., Minster, B., and Michelot, J.-L.: A Newly Designed Analytical Line to Examine Fluid Inclusion Isotopic Compositions in a Variety of Carbonate Samples, Geochemistry, Geophysics, Geosystems, 19, 1107–1122, 2018.

de Graaf, S., Vonhof, H. B., Weissbach, T., Wassenburg, J. A., Levy, E. J., Kluge, T., and Haug, G. H.: A comparison of isotope ratio mass spectrometry and cavity ring-down spectroscopy techniques for isotope analysis of fluid inclusion water., Rapid Communications in Mass Spectrometry, 34, e8837, 2020.

Fleitmann, D., Burns, S. J., Neff, U., Mangini, A., and Matter, A.: Changing moisture sources over the last 330,000 years in Northern Oman from fluid-inclusion evidence in speleothems, Quaternary Research, 60, 223–232, 2003.

Galewsky, J., Steen-Larsen, H. C., Field, R. D., Worden, J., Risi, C., and Schneider, M.: Stable isotopes in atmospheric water vapor and applications to the hydrologic cycle, Rev. Geophys., 54, 809–865, 2016.

Gkinis, V., Popp, T. J., Johnsen, S. J., and Blunier, T.: A continuous stream flash evaporator for the calibration of an IR cavity ring-down spectrometer for the isotopic analysis of water, Isotopes In Environmental And Health Studies, 2010.

Graf, P., Wernli, H., Pfahl, S., and Sodemann, H.: A new interpretative framework for below-cloud effects on stable water isotopes in vapour and rain, Atmospheric Chemistry and Physics, 19, 747–765, 2019.

Gupta, P., Noone, D., Galewsky, J., Sweeney, C., and Vaughn, B. H.: Demonstration of high-precision continuous measurements of water vapor isotopologues in laboratory and remote field deployments using wavelength-scanned cavity ring-down spectroscopy (WS-CRDS) technology, Rapid Communications in Mass Spectrometry, 23, 2534–2542, 2009.

Horita, J., Rozanski, K., and Cohen, S.: Isotope effects in the evaporation of water: a status report of the Craig-Gordon model, Isotopes In Environmental And Health Studies, 44, 23–49, 2008.

Iannone, R. Q., Romanini, D., Kassi, S., Meijer, H. A. J., and Kerstel, E. R. T.: A Microdrop Generator for the Calibration of a Water Vapor Isotope Ratio Spectrometer, Journal Of Atmospheric And Oceanic Technology, 26, 1275–1288, 2009.

https://doi.org/10.5194/amt-2023-55
Preprint. Discussion started: 17 April 2023

Kerstel, E. R. T., Iannone, R. Q., Chenevier, M., Kassi, S., Jost, H. J., and Romanini, D.: A water isotope (H-2, O-17, and O-18) spectrometer based on optical feedback cavity-enhanced absorption for in situ airborne applications, Applied Physics B-Lasers And Optics, 85, 397–406, 2006.

Lee, X., Sargent, S., Smith, R., and Tanner, B.: In situ measurement of the water vapor 18O/16O isotope ratio for atmospheric and ecological applications, J. Atmos. Ocean. Techn., 22, 555–565, 2005.

Lis, G., Wassenaar, L. I., and Hendry, M. J.: High-Precision Laser Spectroscopy D/H and 18O/16O Measurements of Microliter Natural Water Samples, Analyt. Chem., 2007.

McGarry, S., Bar-Matthews, M., Matthews, A., Vaks, A., Schilman, B., and Ayalon, A.: Constraints on hydrological and paleotemperature variations in the Eastern Mediterranean region in the last 140 ka given by the δD values of speleothem fluid inclusions, Quaternary Science Reviews, 23, 919–934, 2004.

Meckler, A. N., Affolter, S., Dublyansky, Y. V., Science, Y. K. Q., and 2015: Glacial–interglacial temperature change in the tropical West Pacific: A comparison of stalagmite-based paleo-thermometers, Quarternary Science Reviews, 127, 90–116, 2015.

Sayres, D. S., Moyer, E. J., Hanisco, T. F., St Clair, J. M., Keutsch, F. N., O'Brien, A., Allen, N. T., Lapson, L., Demusz, J. N., Rivero, M., Martin, T., Greenberg, M., Tuozzolo, C., Engel, G. S., Kroll, J. H., Paul, J. B., and Anderson, J. G.: A new cavity based absorption instrument for detection of water isotopologues in the upper troposphere and lower stratosphere, Review of Scientific Instruments, 80, 044 102–15, 2009.

Seidl, A. W., Sodemann, H., and Steen-Larsen, H. C.: A modular field system for near-surface, vertical profiling of the atmospheric composition in harsh environments using cavity ring-down spectroscopy, Atmospheric Measurement Techniques, 16, 769–790, 2023.

Sodemann, H., Aemisegger, F., Pfahl, S., Bitter, M., Corsmeier, U., Feuerle, T., Graf, P., Hankers, R., Hsiao, G., Schulz, H., Wieser, A., and Wernli, H.: The stable isotopic composition of water vapour above Corsica during the HyMeX SOP1 campaign: insight into vertical mixing processes from lower-tropospheric survey flights, Atmospheric Chemistry and Physics, 17, 6125–6151, 2017.

St Clair, J. M., Hanisco, T. F., Weinstock, E. M., Moyer, E. J., Sayres, D. S., Keutsch, F. N., Kroll, J. H., Demusz, J. N., Allen, N. T., Smith, J. B., Spackman, J. R., and Anderson, J. G.: A new photolysis laser-induced fluorescence instrument for the detection of H2O and HDO in the lower stratosphere., Review of Scientific Instruments, 79, 064 101, 2008.

Steen-Larsen, H. C., Johnsen, S. J., Masson-Delmotte, V., Stenni, B., Risi, C., Sodemann, H., Balslev-Clausen, D., Blunier, T., Dahl-Jensen, D., Ellehøj, M. D., Falourd, S., Grindsted, A., Gkinis, V., Jouzel, J., Popp, T., Sheldon, S., Simonsen, S. B., Sjolte, J., Steffensen, J. P., Sperlich, P., Sveinsbjornsdottir, A., Vinther, B. M., and White, J. W. C.: Continuous monitoring of summer surface water vapor isotopic-composition above the Greenland Ice Sheet, Atmospheric Chemistry and Physics, 13, 4815–4828, 2013.

Steig, E. J., Gkinis, V., Schauer, A. J., Schoenemann, S. W., Samek, K., Hoffnagle, J., Dennis, K. J., and Tan, S. M.: Calibrated high-precision ¹⁷O-excess measurements using cavity ring-down spectroscopy with laser-current-tuned cavity resonance, Atmospheric Measurement Techniques, 7, 2421–2435, 2014.

Sturm, P. and Knohl, A.: Water vapor δ²H and δ¹⁸O measurements using off-axis integrated cavity output spectroscopy, Atmospheric Measurement Techniques, 3, 67–77, 2010.

van Geldern, R. and Barth, J. A. C.: Optimization of instrument setup and post-run corrections for oxygen and hydrogen stable isotope measurements of water by isotope ratio infrared spectroscopy (IRIS), Limnology and Oceanography: Methods, 10, 1024–1036, 2012.

Weissbach, T.: Spectroscopic isotope ratio analysis on speleothem fluid inclusions - analytics and paleoclimatic case studies, Ph.D. thesis, University of Heidelberg, 2020.

https://doi.org/10.5194/amt-2023-55
Preprint. Discussion started: 17 April 2023

Atmospheric Measurement Techniques Discussions

Weng, Y., Touzeau, A., and Sodemann, H.: Correcting the impact of the isotope composition on the mixing ratio dependency of water vapour isotope measurements with cavity ring-down spectrometers, Atmospheric Measurement Techniques, 13, 3167–3190, 2020.